EERA DTOC

THE EUROPEAN ENERGY RESEARCH ALLIANCE
DESIGN TOOLS FOR OFFSHORE WIND FARM CLUSTER

Report on procedure for the estimation of expected net energy yield and its associated uncertainty ranges for offshore wind farms and wind farm clusters

Elena Cantero Nouqueret, Javier Sanz Rodrigo, Sergio Lozano Galiana, Pedro Miguel Fernandes Correia, Giorgos Sieros, Peter Stuart, Tom Young, Ana María Palomares Losada, Jorge Navarro Montesinos, Pedro Ángel Jiménez Muñoz, Matthias Waechter, Allan Morales, Patrick Milan, Charlotte Bay Hasager, Pierre-Elouan Réthoré, Gerard Schepers

31 July, 2013

Agreement n.:	FP7-ENERGY-2011-1/ n°282797
Duration	January 2012 to June 2015
Co-ordinator:	DTU Wind Energy, Risø Campus, Denmark

Support by:

Document information

Document Name:	**Report on procedure for the estimation of expected net energy yield and its associated uncertainty ranges for offshore wind farms and wind farm clusters**
Document Number:	**D3.1**
Author:	**Elena Cantero**
Date:	**31 July 2013**
WP:	**WP3**
Task:	**3.1**

Table of contents

1 EXECUTIVE SUMMARY 6

2 INTRODUCTION 7

3 TEST CASE DESCRIPTION: FINO 1 8
3.1 Instrumentation 8
3.2 Input data 9

4 METHODOLOGY 10

5 METHODOLOGY FROM CIEMAT 13
5.1 Quality Control 13
5.2 Long term 14
5.3 Vertical extrapolation 15
5.4 AEP (P50) 17
5.5 Uncertainty Analysis 17

6 METHODOLOGY FROM CRES 19
6.1 Filtering 19
6.2 Long term 20
6.3 Vertical extrapolation 21
6.4 AEP (P50) 22
6.5 Uncertainty Analysis 22

7 METHODOLOGY FROM RES 24
7.1 Filtering 24
7.2 Long term 24
7.3 Vertical extrapolation 24
7.4 AEP (P50) 25
7.5 Uncertainty Analysis 25

8 METHODOLOGY FROM FORWIND 26
8.1 Filtering 26
8.2 Long term 26
8.3 Vertical extrapolation 27
8.4 AEP (P50) 28
8.5 Uncertainty Analysis 29

9 METHODOLOGY FROM CENER 30
9.1 Filtering 30

9.1.1 General Filters 30

9.1.2 Mast shadowing effect 30
9.2 Long term 32

9.2.1 No long term extrapolation 32

9.2.2 With long term extrapolation 33
9.3 Vertical extrapolation 39

9.3.1 Hellmann exponential law 39

9.3.2 Logarithmic wind profile law 42
9.4 AEP (P50) 43
9.5 Uncertainty Analysis 43

10 FINO 1 VIRTUAL MAST (CENER) 45

11 RESULTS 47
11.1 Filtering 47
11.2 Long term 51
11.3 Vertical Extrapolation 52
11.4 Gross Energy (P50) 53
11.5 Uncertainties and P90 54
11.6 Results from Skiron virtual mast 55

12 FINO 1 TEST CASE DISCUSSION 57

13 AVAILABILITY LOSSES FOR A GENERIC OFFSHORE WIND FARM (RES) 59
13.1 Introduction 59
13.2 SWARM inputs 59
13.3 Definition of '*Excess turbine availability loss*' 60
13.4 Excess turbine availability loss: Results 61
13.5 Conclusions 63

14 O&M TOOLS (ECN) 65
14.1 ECN O&M Tool 65

14.1.1 The Software 65

14.1.2 The Model 65

14.1.3 The Experience 66
14.2 OMCE Calculator 66

14.2.1 The Software 66

14.2.2 The Model 67

15 POWER CURVE DEVIATIONS (FORWIND) 69

16 CONCLUSIONS 70

17 REFERENCES 71

18 ANNEX 1: SENSOR DESCRIPTION 73

1 EXECUTIVE SUMMARY

This report summarizes the methodologies employed by CRES, CIEMAT, RES, Forwind and CENER in the assessment of the Net Annual Energy Production of offshore wind farms and the associated uncertainties.

To analyze the different gross energy estimation techniques in a homogeneous way FINO 1 site has selected as test case. With FINO 1 measured data at different height levels and a power curve as input the participants have calculated mean wind speed, data coverage and wind frequency distribution after filtering; long term wind speed distribution; hub height (120 m) wind speed distribution; long-term predicted gross energy (P50) and the estimated uncertainty of the long term predicted gross energy yield. Participant's results were independently compared and contrasted with one another.

In order to analyze the mesoscale outputs as offshore virtual masts the gross annual energy production has been calculated with data from nearest grid point of Skiron mesoscale model and added to the results comparison.

The results are discussed within this report, as conclusion the need of clear and common methodologies and standards to do the wind energy yield assessment in offshore wind farms and data to validate them.

To obtain Net Annual Energy Production from Gross Annual Energy Production different losses must be estimated.

RES has done a general analysis of percentage yield lost due to weather window accessibility for a range of wind farm parameters. They have estimated the energy-based Turbine Availability loss for a generic 600 MW offshore wind farm for a number of scenarios, using the RES software SWARM.

ECN presents its O&M Tool (Operation and Maintenance) which has been developed to estimate the long term annual average costs and downtime of an offshore wind farm; and the OMCE-Calculator (Operation and Maintenance Cost Estimator) developed to estimate the future O&M costs of an operating offshore wind farm.

Forwind discussed the power curve deviations between manufacturer and on-site power curves in offshore sites due to reduced levels of vertical shear and turbulence intensity.

Finally conclusions and good practices will be stated and recommendations on future effort and investigation given.

2 INTRODUCTION

The purpose of this report is to describe the work undertaken and the results within work package 3 (WP3).

The aim of WP3 consists of providing means to produce an accurate assessment of the expected net energy yield from wind farms and clusters of wind farms as well as the associated uncertainty by integrating results from work package 1 (WP1) and work package 2 (WP2).

This work package aims to checking methodologies and techniques used in the assessment of the Net Annual Energy Production of offshore wind farms and the associated uncertainties. Given the lack of available data from operational wind farms it is challenging to validate the proposed methodologies, especially regarding uncertainty quantification which is very case-specific.

3 TEST CASE DESCRIPTION: FINO 1

This description has been prepared for EERA-DTOC WP3 activities and presents the main characteristics of FINO 1 research platform, which is situated in the North Sea, approximately 45 kilometres off the Borkum Island (Figure 3.1.1), at a depth of some 30 meters. The exact site coordinates are as follows:

N54° 0.86´ E6° 35.26´

FINO 1 data can be used as test case for estimating Gross Energy in a hypothetical wind farm.

The FINO 1 platform operates unattended under harsh environmental conditions offshore. To meet the different requirements of all users, BSH (Bundesamt für Seeschifffahrt und Hydrographie) provides as much data as they can get. Distorted or abnormal measurements are not excluded as long as it is not proven that they are clearly erroneous. The specifications of the measurement set up provided in this document have been extracted directly from [3.1] sent by BSH. More detailed information about the FINO 1 mast and wind conditions can be found in [3.2].

Figure 3.1.1: Location of FINO1 research platform

3.1 Instrumentation

The database accessible from this website [3.3] contains the results of comprehensive meteorological and oceanographic measurements made at the offshore test field, as far as they have become operational.

The height of the measurement mast is 100m. Seven cup anemometers are installed at heights of 30 m to 100 m on booms mounted in southeast direction of the mast. One cup anemometer is mounted on top of the mast at 100m height. Three ultrasonic anemometers are present at heights of 40 m, 60 m, and 80 m on north-westerly oriented booms (Figure 3.1.2). Additional meteorological measurements consist on wind direction, air temperature, moisture, air pressure and solar irradiation. The oceanographic measurements include waves, wave height, water current and physical properties of the sea water. A detailed sensor description is provided in ANNEX 1.

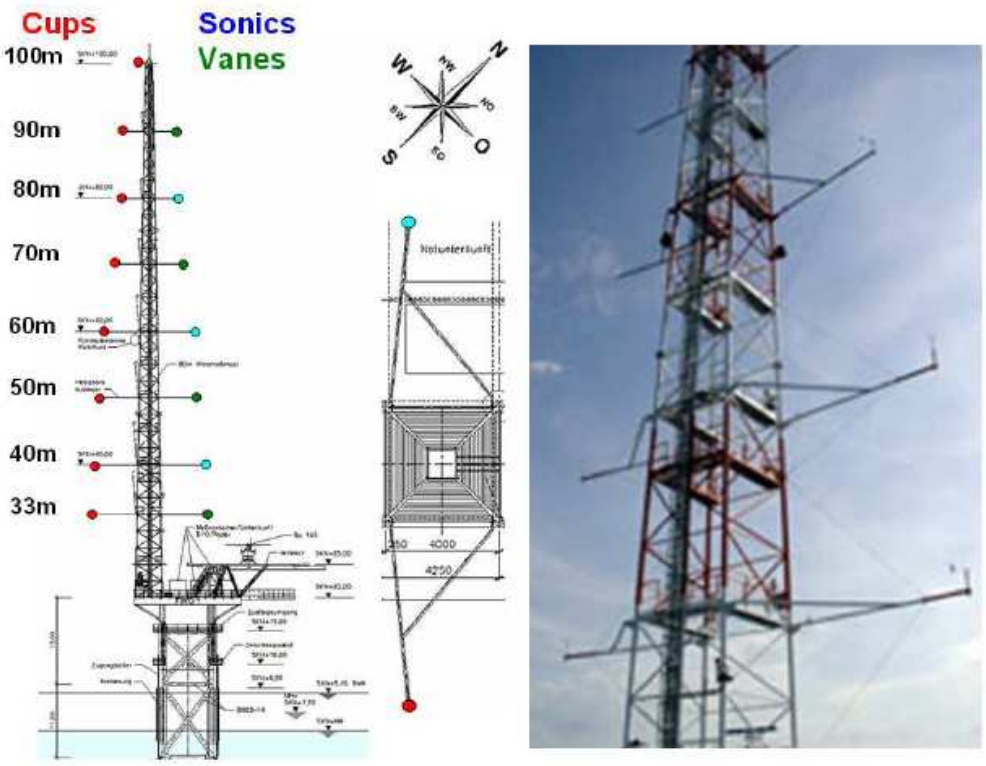

Figure 3.1.2: Location and orientation of FINO1 sensors

Mast shadowing effects need to be considered because of the high distortion effects expected from such a large tower on the anemometers. Figure 3.1.2 shows the orientation of the sensor booms with respect to the tower. Flow distortion is also present at the top-mounted anemometer since it is surrounded by lighting rods at E, W, N and S directions.

3.2 Input data

The following data was provided for the AEP comparison based on 10-minute averaging period:

- Time series of controlled[1] measured mean, standard deviation and maximum wind speed, mean and standard deviation of wind direction, temperature and pressure.

- Generic power and thrust curves as well for a 2 MW wind turbine, with 80 m rotor diameter and 120 m hub-height, based on an air density of 1.225 kg/m^3. For the purpose of this test and to avoid dispersion in air density estimation, the mean site air density shall be assumed to be 1. 225 kg/m^3.

[1] DEWI, the institute that is in charge of the meteorological measurements at FINO1, controls the data and correct them if necessary.

4 METHODOLOGY

In order to provide an accurate value of the expected net energy yield, the offshore wind resource assessment process has been reviewed (Figure 4.1) as well as the sources of uncertainty associated to each step.

The gross annual energy prediction (AEP) is derived from either measured or virtual (simulated) wind speed time series at hub-height, U_{hub}, integrated over long-term period together with the power curve from the target wind turbine. Observations need to be filtered out of spurious registers and eventually require vertical extrapolation to hub-height. In the absence of onsite measurements, virtual time series generated by a numerical weather prediction (NWP) model and interpolated to the site and height of interest are used. Long-term extrapolation against historical observational or virtual data is necessary if the original period is of short duration.

The net annual energy production (AEP_{NET}) is the result of applying various sources of energy inefficiency to the AEP, notably: from wind farm wake losses, from electrical losses, from unavailability losses during operation and maintenance (O&M) activities. Wake efficiency is the object of WP1 while the electricity losses are characterized in WP2.

Alongside the process of AEP_{NET} assessment we need to take into account the different sources of uncertainty (Δ) that are propagated in each step. The final outcome of the process is probabilistic with a probability density function defined in terms of the 50, 75 and 90% percentiles (P50, P75, P90). These outputs are used by financial models to calculate the expected return of investment of the project. In brief, the project is more profitable with increasing P50 and less risky with decreasing P90/P50 ratio.

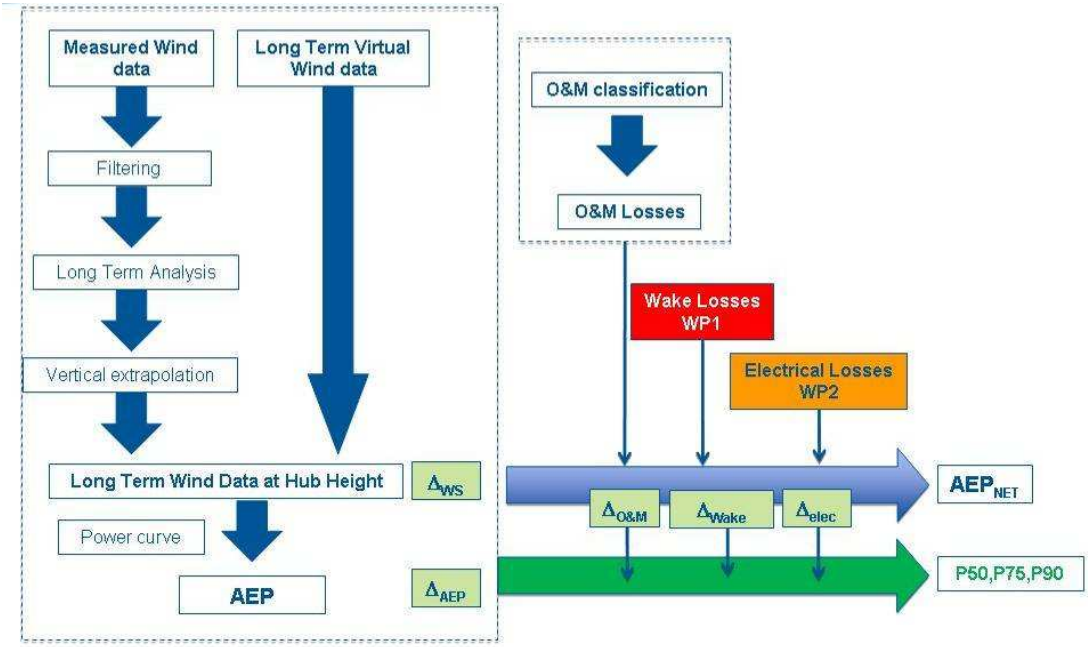

Figure 4.1: The main components in a offshore wind resource assessment

Based on FINO 1 input data CRES, CIEMAT, RES, Forwind and CENER have estimated the Gross Annual Energy production using own methodologies. To analyze the different techniques in a homogeneous way, the next information has been requested to each participant:

1. For each measured level (100, 90, 80, 70, 60, 50, 40 and 33 m) the mean wind speed for the measured period to make sure that all participants have the same input.

2. To check the filtering techniques and their impact on the results: mean measured wind conditions after filtering: mean wind speed and data coverage for each height level, wind frequency distribution of hours in the year as a function of wind speed and direction for the 100 meters level and mean turbulence intensity at 100 m.

3. Long term wind speed distribution and turbulence intensity as a function of wind direction sector at 100 m level. Long term reference data is not provided as an input such that each participant can use own reference information (meteorological station or virtual data from databases like MERRA, GFS, World Wind Atlas Data…); this will allow assessing the impact from different reference data sources and Measure-Correlate-Predict (MCP) methods of temporal extrapolation.

4. Vertical extrapolation techniques of the mean wind speed and turbulence intensity will be analyzed for a prediction height of 120 meters.

5. AEP will be analyzed based on the long-term prediction of gross energy yield in GWh/year, before wake effects and any other losses.

6. The estimated uncertainty of the long term 10-year equivalent predicted gross AEP, including a breakdown of the individual uncertainty components that have been estimated or assumed.

7. Details of how the particular methodology of each participant, in particular on how the wind speed prediction has been carried out (e.g. MCP technique), if measured or modeled wind shear was used, etc.

To analyze the NWP outputs as offshore virtual masts the gross annual energy production has been calculated based on data from nearest grid point of Skiron mesoscale model simulations.

The wake effects between wind turbines are particularly relevant in offshore environments where long periods of atmospheric stability conditions make the flow recover more slowly than in onshore conditions. This information is obtained from WP1 and it is of great importance at estimating the net energy yield.

Secondly, any cluster of wind farms involves a considerable electrical infrastructure that inherently will produce a certain amount of electrical losses inside each wind farm, between wind farms inside the cluster and between the cluster and the shoreline. The procedure for the estimation of these losses can differ considerably from those at onshore sites and must also be estimated as accurately as possible. This information is obtained from WP2.

Thirdly, an important factor to be included at the net energy yield estimation is the availability of wind turbines and wind farms. Availability of wind farms can be affected by the combination of the vulnerability of wind farm design, weather conditions, wind turbines degradation and maintenance infrastructure. Availability data of wind farms at different scenarios and climatology are not available so a general analysis of percentage yield lost due to weather window accessibility for a range of wind farm parameters will be done by RES. The considered parameters are:

- Significant wave height limit (between 1.0 meters and 2.0 meters)
- Distance from shore
- Wave conditions (benign, moderate and severe)

The objective of this work package is to estimate the expected energy loss due to wind farm accessibility depending on the topology and location of the clusters of wind farms.

The structure of the report is to take each project partner's explained its wind resource assessment methodology, then to discuss the FINO 1 test case results and synthesis the different methods and results. The general analysis of percentage yield lost due to weather window accessibility for a range of wind farm parameters will be explained. Finally conclusions and good practices will be stated and recommendations on future effort and investigation given.

5 METHODOLOGY FROM CIEMAT

On the basis of data provided in the FINO1 research platform, CIEMAT has conducted a series of steps with the main objective to obtain the Gross Energy (P50) and an estimation of its uncertainty (P90). To achieve these objectives we have separated the study in the following structure: Quality Control, Long term, Vertical extrapolation, Gross Energy (P50) and Uncertainty Analysis.

5.1 Quality Control

The Quality Control procedure developed in the present study and applied to the observational wind dataset is structured in three main steps that involve the detection and suppression of rough errors: 1) manipulation errors (such as artificial data repetitions); 2) unrealistic values in wind speed and direction; 3) abnormally low (e.g. long periods of constant values or calms) and high variations (e.g. extreme values). Furthermore, although no homogenization tests have been applied, an inspection and correction of systematic errors have also been performed in a fourth step. The wind speed and wind direction data are assessed independently, although most of the steps are common for both variables. Most of the techniques applied are based on previous works by CIEMAT [5.1]. However, it is worth emphasizing that each observational database presents particular quality problems and requires specific treatment.

The mean wind speed and percentage of remaining data after filtering for each height of measurement is presented in the Table 5.1.1. The percentage of data with which we are going to work is greater, in virtually all levels, than 96 %.

Table 5.1.1: Mean wind speed and percentage of data for 100, 90, 80, 70, 60, 50 and 40 meters above ground level.

Anemometer	Mean wind speed [m/s]	Percentage of remaining data after filtering [%]
V100	9.84	96.55
V90	9.40	96.52
V80	9.32	95.50
V70	9.20	96.60
V60	9.09	96.60
V50	8.89	93.00
V40	8.66	90.87
V33	8.49	89.79

5.2 Long term

The annual temporal evolution of the mean wind speed at FINO 1 database is shown in Figure 5.2.1. For the level of 100 meters, the year with less wind was 2010 (9.00 m/s) and the windiest years were 2007 (10.20 m/s) and 2008 (10.25 m/s). The variability with respect to the mean value of each of the annual means is smaller than 9 %. The box-plot of the wind speed (Figure 5.2.2) reveals a clear annual evolution. The winds are stronger in winter than in summer. During the summer, the monthly distributions are more similar. The change in the trend at 50 meters above the ground level in the year 2008 (yellow line in Figure 5.2.1) should be studied, although it is not subject to this analysis.

The time length of the FINO 1 database is from 13/01/2005 to 01/07/2012 for this analysis we have used data from 2005 to 2011 to take into account full years. The only year with missing data in more than a moth is 2012.

In the wind energy sector, the life-time of the park is considered to be around 20 years. The wind data do not usually have a tendency and the mean wind at a site is fairly stable in time, from a certain number of years. In our case, only taking into account 4 years the variability in the wind mean is less than 2 %. We have therefore considered that the average wind speed of the 7 years studied can be considered a good estimation of the long term mean and it has been applied only an increase it by 2% due to FINO 1 mast correction [5.2].

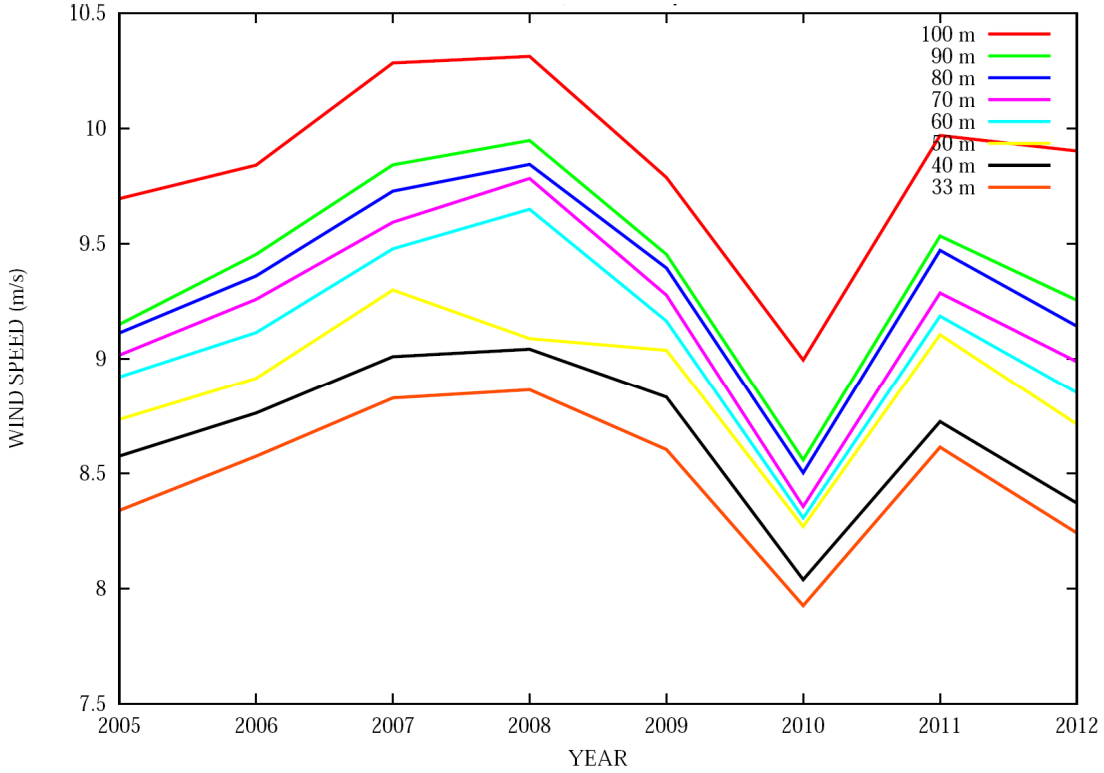

Figure 5.2.1: Annual wind speed at the different heights (see legend).

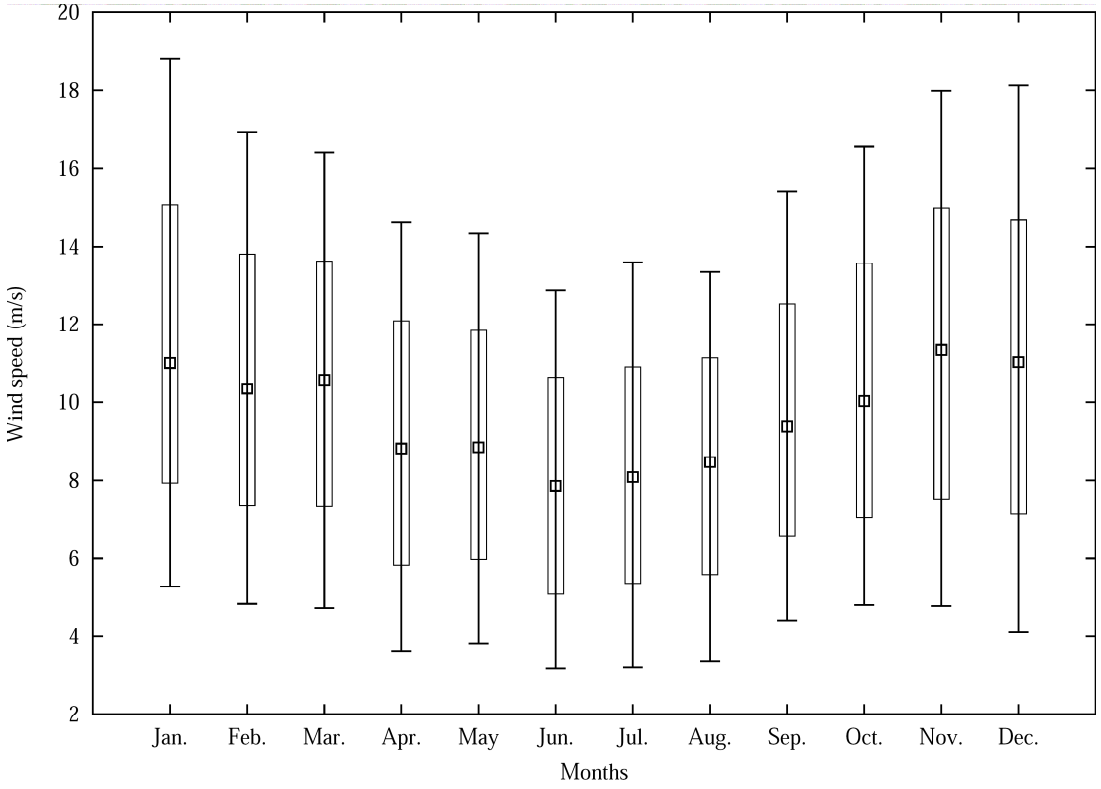

Figure 5.2.2: Box and whiskers plots, FINO 1 100 meters about ground level, showing the distribution of the mean wind speed field for each Month. The central square indicates the median, the lower bases of the boxes are the 25 percentiles and the upper ones the 75 percentiles. The lower and upper whiskers indicate the 10 (lower) and 90 (upper).

5.3 Vertical extrapolation

In order to calculate the vertical extrapolation a wind shear profile in power law has been used.

$$\frac{U_2}{U_1} = \left(\frac{z_2}{z_1}\right)^{\alpha}$$

Where α (alpha) is the surface roughness exponent, shear exponent, power law coefficient, etc… that can be obtain by the velocity at two levels.

The main objective is to estimate the wind velocity at 120 meters height above ground (sea) level from the wind speed at 100 meters. In Figure 5.3.1 CIEMAT has presented the surface roughness exponent (alpha) in function of height above ground level in the FINO 1 mast. There is an overestimation for the 100 meters above ground level (100/90).

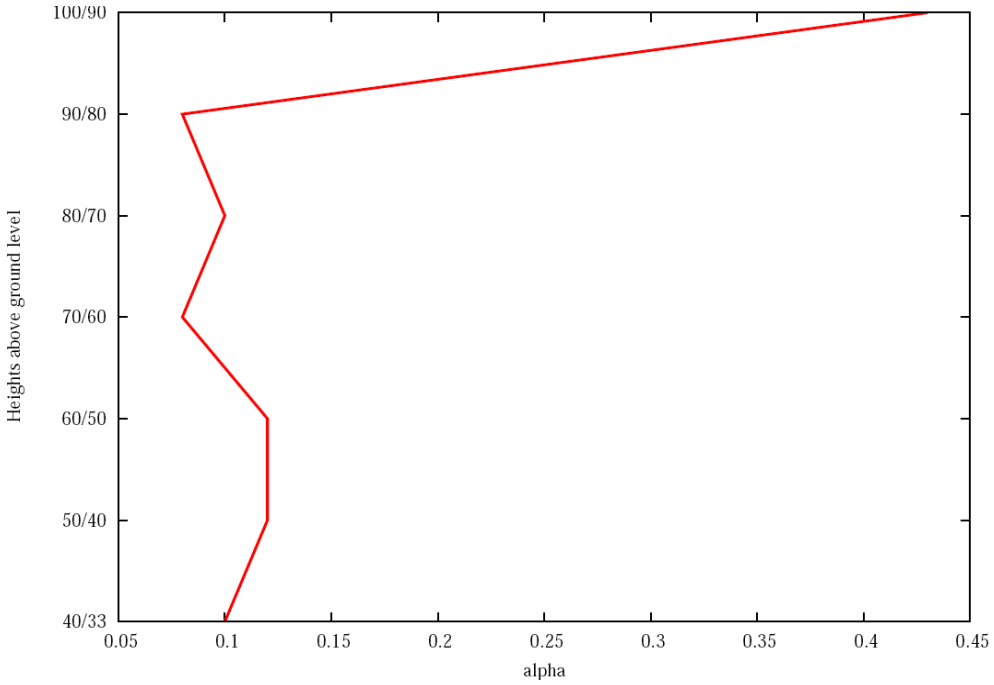

Figure 5.3.1: The surface roughness exponent versus ratio of heights above ground level.

This anomaly value may be due to the presence of the tower itself. Figure 5.3.2 shows the 90 meters above ground level wind direction distribution (there is not a wind direction sensor installed at 100 m) of the alpha coefficient (ten minutes averaged) for the wind speed at 100/90 m above ground level. There is an interval of around sixteen degrees (280° – 340°) in which alpha has larger values. Since alpha is usually near to 0 this higher value strongly affects the mean value. This effect is related to the lightning protection cage and the installation of the tower itself [5.2].

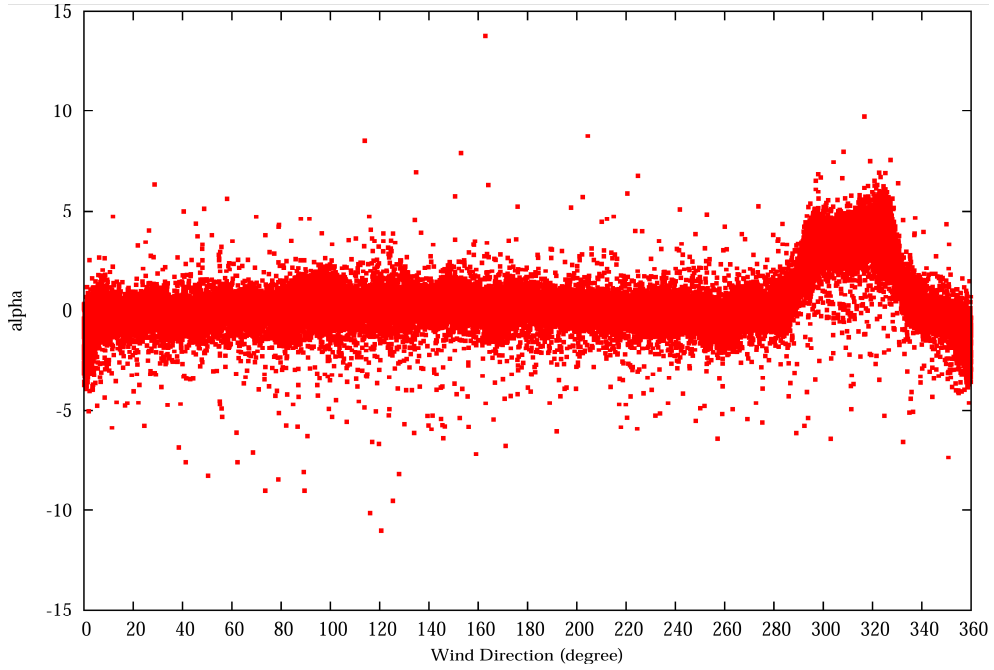

Figure 5.3.2 : The wind direction versus alpha coefficient (100/90 heights above ground level).

The value of alpha is around 0.07 if we remove the wind velocity for the perturbed directions. However, how we do not have a measure of the wind direction to 100 meters height, therefore we cannot 'clean' the inference of the tower in the wind data in this height. Alpha decreases with the height and a typical value for unstable air above open water surface is 0.06, a conservative value of 0.03 has been chosen..

5.4 AEP (P50)

The extrapolated wind speed and the power curve provided by the manufacture have been used to calculate the gross energy production in a typical year (P50). In this case no air density correction has been done and a value of 1.225 kg/m^3 has been used.

In particular, the annual gross energy (P50) have been calculated using the following formula:

$$\text{Gross Energy yield} = \sum \text{Prob}(Ui) * \text{Power}(Ui) * 8760\ h = 10{,}64\ GWh$$

Where *i* correspond to each bin of velocity.

5.5 Uncertainty Analysis

The following typical values for the uncertainties have been taking in account:

- **Wind measurement**, mast flow distortion: This uncertainty source arises when measuring the actual wind speed at the site. Several factor can contribute to errors in the measurement of wind speed, and therefore in the determination of mean wind speed. These factors fall into the category of wind speed measurement uncertainty (calibration uncertainty, dynamic over speeding, vertical flow effects, vertical turbulence effects, tower effects, boom and mounting effects and data reduction accuracy). For this case a typical uncertainty, according to our experience in offshore wind farms, of 1.96% is used.
- **Deviation from future (10 years)**: This uncertainty source arises when the measured wind resource data are used to estimate the long-term wind resource at a site. Typically, twenty years is assumed to be a long enough time period to characterize the long-term wind resource. A typical uncertainty, according to our experience in offshore wind farms, of 1.50% is used.
- **Deviation from historical**: The actual wind resource over the timelife of the turbine may not be the same as the true long-term wind resource, which produces additional uncertainty, in this case a typical uncertainty, according to our experience in offshore wind farms, of 1.50% is used.
- **Extrapolation horizontal**: The reference site data used in the called Measure-Correlate-Predict to estimate the long-term parameters might not in fact be representative of the true long-term values, for this reason a typical uncertainty, according to our experience in offshore wind farms, of 1.00% is used.
- **Power curve**: The three sources of power production uncertainty are: Wind turbine specimen variation, wind turbine power curve variation and air density uncertainty. For this case a typical uncertainty, according to our experience in offshore wind farms, of 1.75% is used.

A sensitivity factor has been used to translate the wind speed uncertainties to production uncertainties. A typical value for an offshore wind farm is 1.02 and is the value that has been used in this study. Other factors of uncertainty that we can take into account for % of P50 energy that are not considered in this analysis are turbine availability, blade dirt & icing, Electrical losses, high-wind hysteresis, array, grid availability, etc...

CIEMAT used the root-sum-square to integrated the independent sources of uncertainty into the total uncertainty, $\varepsilon = (\varepsilon_i^2)^{1/2}$. Where *i* is each source of uncertainty.

P90 was interpreted as the energy production that should be expected with a probability 90% and was calculated as the 10% quantile of a Gaussian distribution with mean value P50 and standard deviation ε.

6 METHODOLOGY FROM CRES

6.1 Filtering

The process of filtering the available data consists of automatic and user-applied filters. It is important to ensure that we do not discard more than the required Filtering is based on the following:

- Direction:
  - Discard more than 3 consecutive identical measurements (frozen/stuck vane)
  - Discard measurements where direction SDV = 0 (frozen/stuck vane)
  - Discard measurements where direction SDV is unavailable
  - Discard measurements where direction differs by > 35 degrees from the average of the other vanes
- Speed
  - Discard measurements where velocity SDV = 0
  - Discard measurements where velocity SDV is unavailable
  - Discard measurements where there is no valid direction (as there are multiple vanes this was relaxed so as not to require the direction at the equivalent height to be present. Forcing this would discard a lot of measurements at some heights (40 m) where the direction data is missing, while direction data at other heights is available. Given that the correlation between heights was generally excellent, these speed measurements were retained with directions filled in from other heights)
  - Discard measurements where the ratio of velocities at different heights exceeds prescribed limits. A problem with this is that because of the direction of the booms at other heights the ratios are irregular around the NW direction (see Figure 6.1.1). Applying the filter would discard the (correct) measurements at 100 m, as they appear incompatible with the (incorrect) measurements at other heights. For this reason and since the 100 m measurement is the one of real interest, a very large range was allowed, leading to practically zero filtering.
  - Discard measurements where maximum velocity (gust) < average velocity (error)

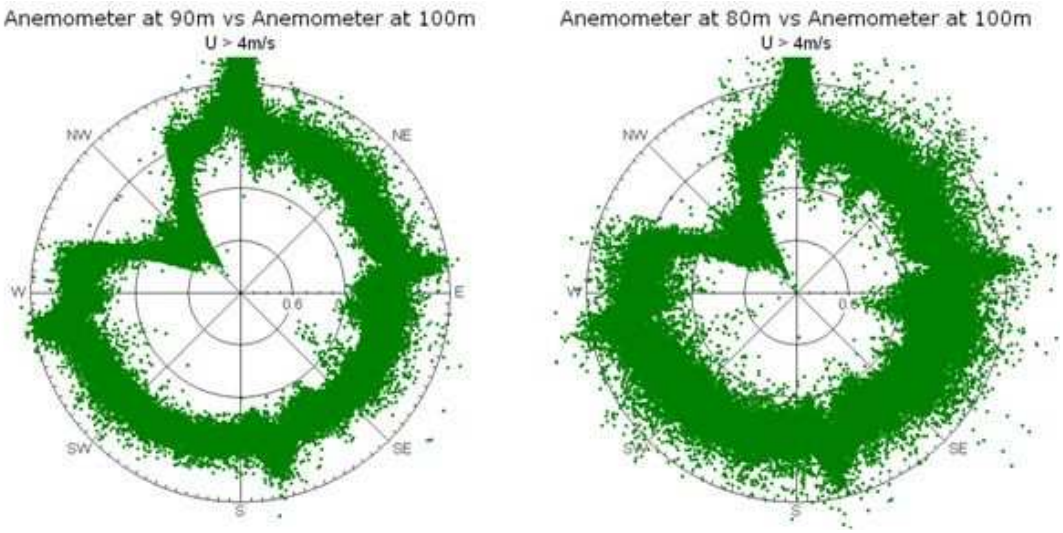

Figure 6.1.1: Ratio of velocities at different heights of the FINO 1 platform, plotted for direction.

The final result of the filtering process is summarised in the Table 6.1.1.

Table 6.1.1: Filtering of the mast data.

Anemometer	Mean wind speed [m/s]	Percentage of remaining data after filtering [%]
V100	9.87	90.70
V90	9.45	90.70
V80	9.38	89.75
V70	9.25	90.80
V60	9.15	90.80
V50	8.99	88.80
V40	8.76	85.85
V33	8.61	86.40

6.2 Long term

With the given measurements covering >7 years we would *NOT* use any kind of long term correction, unless it comes from a very close mast with a correlation coefficient of > 95%. In any other case the added uncertainty is higher than the gain. The only data that was available to CRES was the NCAR predictions at the nearest station. Using MCP resulted in poor correlation to the existing dataset and was not used. A correction based simply on monthly averages was applied in the results (the effect is negligible, dropping the wind speed at 100 m from 9.87 to 9.85 m/s).

We stress that in a real application with > 7 years available we would not use any correction. A statistical analysis, based on individual events, shows that the uncertainty range as a function of the Weibull coefficients and the duration of the measuring campaign follows the trend of the Figure 6.2.1, where for k=2 and 7 years the uncertainty has dropped to ~2%.

Using an MCP correlation will almost invariably introduce a higher uncertainty, unless we have access to a mast in the same wind farm.

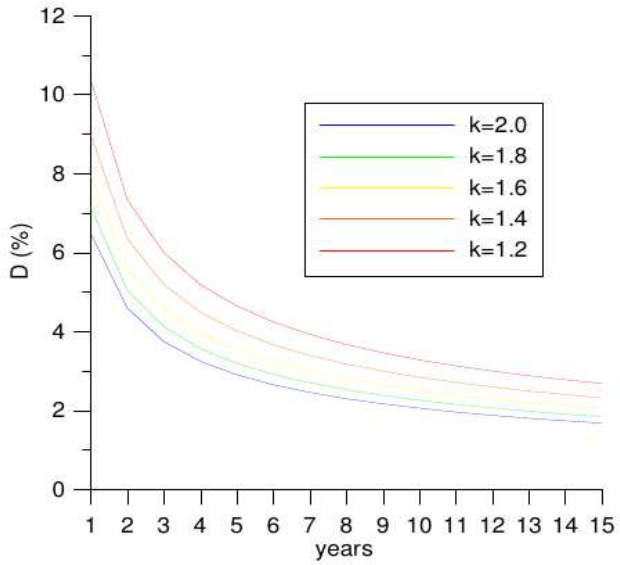

Figure 6.2.1: Uncertainty of the mean of ten-minute averaged wind speeds as a function of the measurements duration and the Weibull form factor k. Confidence level 95%.

6.3 Vertical extrapolation

For the derivation of the time series at 120 m, the exponents of the power law were calculated independently for 12 sectors (the average value is ~0.09), based on the measurements. The two sectors at 300 and 330 degrees had poorer correlations, affected by the boom orientation that distorts the speed measurements. This effect is obvious in the relative Figure 6.1.1 of the velocity ratios. It is also worth pointing out the effect on turbulence intensity (see Figure 6.3.1), where the values for 80, 90 and 100 m are similar except for the affected sector, where the intensity increases for the two lower heights. For this reason the shear coefficient was calculated neglecting the 100 m measurement for two of the sectors. Based on the calculated values a “dummy” time series at 120 m is produced.

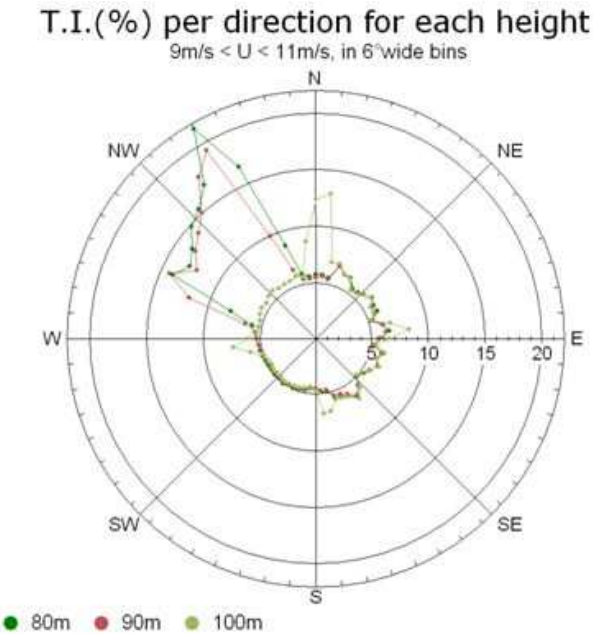

Figure 6.3.1: Turbulence intensity per direction for the three highest anemometers

6.4 AEP (P50)

We generally employ one of three (theoretically equivalent) methods to estimate the gross yield, based on the power curve:

1. Integration of the actual time series with the power curve provided
2. Use of the wind rose at the relative position
3. Use of sector-wise Weibull distributions at the wind turbine position(s).

The method used for this particular application was the first one. A 0.7% production loss was calculated as a result of hysteresis (operation between cut-off and re-cut-in) based on the given characteristics. It should be pointed out that no density correction was performed for the power curve, in order to keep the results comparable, but in real conditions a correction would be made based on either local measured temperature or a long-term estimate for the temperature.

The result for the energy yield was 9.85GWh/year, corrected to 9.79GWh/y when considering the non-uniform distribution of missing data around the year.

6.5 Uncertainty Analysis

The following uncertainties have been taking in account:

- **Wind Speed Measurements**, details for the wind speed measurements that were used in this study are now known. It is assumed that they were carried out by an accredited for wind potential measurements organization and a typical uncertainty of 2.0% is used. Detailed calibration sheets would be needed for a more accurate assessment.
- **Long-term Wind Speed Variability**, this is based on statistical analysis of the available measurements. As the period covered is >7years the resulting uncertainty is small
- **Wind Data Horizontal and Vertical Extrapolation**, horizontal extrapolation is not considered, as it is assumed that the wind turbine operates at the mast position. For the vertical extrapolation the measurements from 40-90 m are used to derive the power law coefficients and the error margin on those. Uncertainty is calculated based on this error margin.
- **Power Curve**, a 5% uncertainty was attributed to the power curve. Depending on the contract signed by the Company and the Manufacturer the guaranteed performance is often based on the uncertainty of the measured power curve (if such a measurement is performed), which is not known beforehand. Therefore this particular uncertainty is subject to verification.

Uncertainties related to wake losses and availability are not considered for the gross production (they are included in the final net production estimate for a given wind farm).

Power estimate was based on a fixed density, as per the instructions for the case. Normally we would correct for local temperature/density.

The uncertainties related to wind speed are multiplied by the **sensitivity factor** to translate them to production uncertainties.

The **wind speed sensitivity factor** (i.e. the change in energy production for a unitary change in wind speed) is calculated from the power curve of the wind turbine. For the numerical estimation of the sensitivity factor, the production is calculated for mean speeds that differ from the reference one by ±2% and the effect on energy production is calculated. Due to the high wind speed the sensitivity is lower than one would typically expect for an onshore wind farm (1.029).

Table 6.5.1 summarizes these uncertainties.

Table 6.5.1: Summary of uncertainty calculations

Source of uncertainty	m/s	% of mean wind speed	GWh	% of P50
Measurement uncertainty	0.20	2.00%	0.20	2.05%
Long Term uncertainty	0.13	1.31%	0.13	1.34%
Vertical Extrapolation	0.17	1.70%	0.17	1.74%
Horizontal Extrapolation	0.00	0.00%	0.00	0.00%
Power Curve			0.49	5.00%
Total			**0.57**	**5.84%**
P90			**9.11**	**92.50%**

7 METHODOLOGY FROM RES

7.1 Filtering

The data was first quality-controlled to remove any periods of bad or missing data. Reasons for data removal included anemometers flat-lining (sticking at a constant wind speed reading), dropping out to zero wind speed, or other erratic behaviour such as wind speed spikes. No clear evidence of anemometer icing was found.

The 103 m anemometer is affected by the lightening cage. By plotting the ratio of the 103 m and 92 m wind speeds, four distinct peaks can clearly be seen in the NE, SE, SW and NW sectors. The effects of this cage were removed as much as possible by fitting Gaussian profile to each of the four affected regions and correcting the wind speed time series for the 103 m anemometer.

7.2 Long term

The long-term mean wind speed at the 103 m anemometer was estimated using the measure-correlate-predict methodology. The nearest MERRA node point was used as a reference data source and was found to be correlated extremely well with the FINO data (r = 0.93). A matrix method was used to define the correlation between the two data sources.

In order to derive the long-term mean wind speed, RES derived two different estimates and then combined them. These are described below:

1. An 'Annual Average Estimate' (AAE): This is the mean wind speed from the FINO 1 data alone, corrected for seasonal bias, with no long-term reference source. The AAE for the 103 m anemometer covered the period 13/01/2005 to 01/07/2012.
2. An 'Historic Estimate' (HE): This is the mean wind speed predicted from the MERRA data after applying the correlation, for the period 12/01/1996 to 12/01/2005.

The AAE and the HE represent two separate estimates of the long-term wind speed at the FINO 1 mast. The final long-term mean wind speed was estimated by calculating a weighted-average of the AAE and the HE. However, it is worth noting that in this case, the AAE and HE were actually identical, i.e. the mean wind speed during the measurement period was the same as in the historic reference period.

The long-term wind frequency and directional distributions were taken directly from the measured data, after correcting for seasonal bias. RES believed that with seven years of measured data, the measured distribution would be more representative of the site than using the MERRA data.

It should be noted that due to the top anemometer being stub-mounted, RES would usually add a correction to reduce the mean wind speeds, because it is common for such anemometers to overestimate the wind speed. However, in this case there was insufficient information about the anemometer setup to decide what correction should be applied. Therefore, instead of adding a correction the anemometer measurement uncertainty was increased as described in the Uncertainty Analysis section below.

The turbulence intensity at 103 m was calculated directly from the 103 m wind speeds and standard deviations.

RES used the full period of data provided from FINO 1 for this assessment. Although the Alpha Ventus wind farm was constructed during the measurement period, RES have ignored the effect of this in the analysis because it was not mentioned in the instructions for the test case.

7.3 Vertical extrapolation

The wind shear exponent was calculated using the ratio of the measured wind speeds between the anemometers at 91.5 m and 71.5 m. The 103 m anemometer was not used for the shear calculation because it is stub-mounted.

There was a strong tower-shadow effect on this mast. RES removed this effect from the shear calculation by fitting a Gaussian profile to the affected area and correcting the wind speed ratios.

Both the 'exponent of means' and 'mean of exponents' methods gave very similar results in this case. The 'exponent of means' was used in the final result because it gave a slightly lower (more conservative) estimate of the hub height wind speed.

The turbulence intensity measured at 103 m was vertically extrapolated to hub height by assuming that the wind speed standard deviation remains constant with altitude [7.1]. The turbulence ratio between measurement height and hub height was therefore the inverse of the wind speed ratio.

7.4 AEP (P50)

Since no wake model or horizontal extrapolation was required for this analysis, deriving the gross energy was relatively simple. The turbine power curve was combined with the predicted long-term wind distribution to produce the gross energy yield, using RES software.

The precise definition of Gross Energy can vary between organisations. Therefore, RES have also derived the energy yield accounting for high wind speed hysteresis loss. This was calculated using our internal software.

7.5 Uncertainty Analysis

The ten-year uncertainty in the gross energy yield was calculated as a combination of the following components:

- Uncertainty in the vertical extrapolation
- Uncertainty in the long term mean wind speed estimate
- Uncertainty in the turbine power curve
- Uncertainty in the mean air density

The two largest uncertainty terms were the wind speed and power curve uncertainties. These terms dominated the overall uncertainty value. This is partly because with only a single turbine there is no possibility for power curve variation to average-out across the wind farm.

The uncertainty on the long term mean wind speed is itself made up of a number of component uncertainties, including:

- **Instrumentation uncertainty**. This was increased above the usual value because the 103m anemometer was stub-mounted and surrounded by a lightening cage. An extra uncertainty term was added to account for this.
- **MCP uncertainty**: This is the uncertainty associated with the MCP process including determining the correlation between the FINO mast and MERRA data.
- **Historic and AAE uncertainties**: These are the uncertainties that arise from assuming that the historic data period and the measurement period are representative of the long-term wind speed at the mast and from the removal of seasonal bias.
- **Future wind speed uncertainty**: This is the uncertainty caused by the natural variability of the wind year-to-year. The future uncertainty was derived assuming a ten-year future averaging time.

An inter-annual variation in mean wind speed of 6% was assumed for the uncertainty analysis.

8 METHODOLOGY FROM FORWIND

8.1 Filtering

For the filtering of the FINO 1 measurement data the strategy was chosen to discard unreliable data instead of attempt a correction in the disturbed data. Three criteria were used for filtering the data. For all cup anemometers only data before 2009-07-14 was used, which means only data before the construction of Alpha Ventus was considered. For the 103 m cup anemometer the lightning shielding was taken into account, therefore wind coming from the four cardinal directions was discarded (e.g., wind between 80 and 100 degrees was discarded). For the cup anemometers on lower height levels only data of the sector between 0 and 280 degrees was considered. Figure 8.1.1 shows the difference between the wind speed measured at 103 m and the wind speed measured at 90 m. The effects of the tower around 300° and of the lightning protection at 0°, 90°, 180°, and 270° are clearly seen.

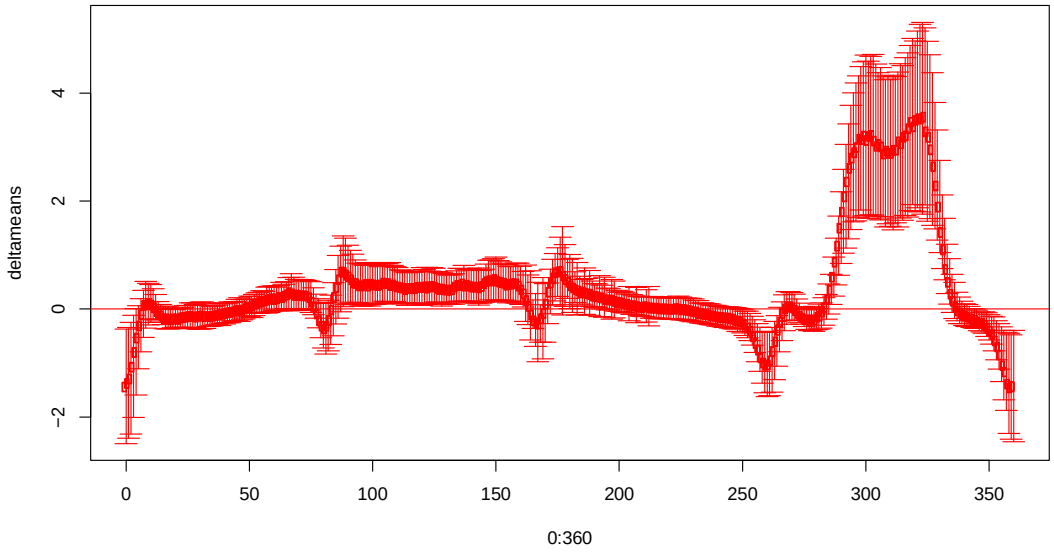

Figure 8.1.1: Difference of the wind speeds measured at 103 m and 90 m of the FINO 1 platform, plotted as averages and standard deviations in bins of one degree width. The tower shadow on the 90m anemometer is clearly visible between 280 and 340 degrees. At the cardinal directions of 0, 90, 180, and 270 degrees the influence of the lightning protection on the top anemometer generates further deviations.

8.2 Long term

The long term predicted wind speed was estimated based on a Measure-Correlate-Predict (MCP) method. NCEP reanalysis data was used as a long term reference. Data from 1979 to 2011 have been used. The correlation between the filtered data of FINO 1 and the long term reference was derived for each wind direction sector. Figure 8.2.1 shows an example of the correlation between FINO 1 and the reference data for monthly averaged wind speed. The figure shows results of one directional sector. Note that the sectors were selected according to the direction of the reanalysis data. From the correlation a linear fit is performed to the data. This linear relationship between FINO 1 and reanalysis data is then used to extend the FINO 1 measurements into a long-term predicted wind time series.

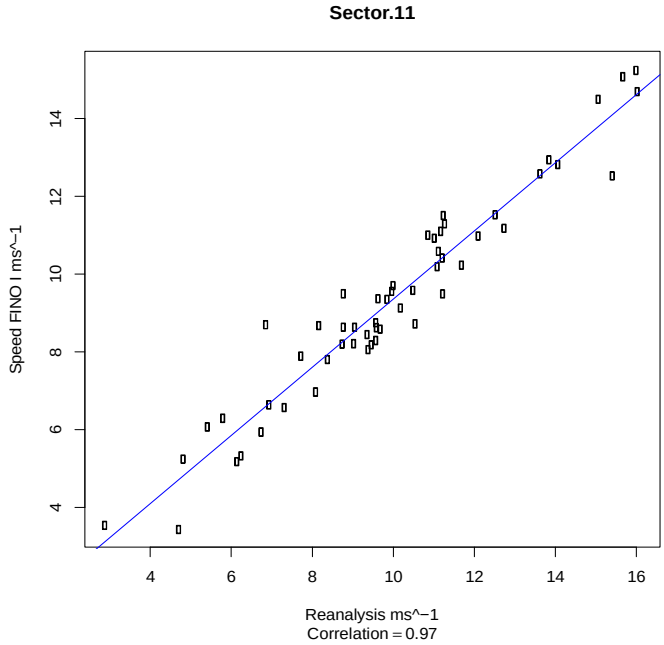

Figure 8.2.1: Example of regression analysis between long-term data and filtered FINO 1 measurements for one directional sector.

8.3 Vertical extrapolation

The long term predicted wind speed time series was vertically extrapolated from 100 m to 120 m according to measured wind profiles. The wind profiles were estimated for three different seasons or the year. The seasons were partly selected using monthly wind indexes as reported in the literature [8.1] for FINO 1. Only data in the sector between 220° and 230° was used for the estimation of the wind profiles. This directional sector is considered to be free of mast obstruction [8.2]. However the profiles were corrected for overspeed effects following a similar procedure as in [8.2] with the cup anemometer at 103 m, see Figure 8.3.1.

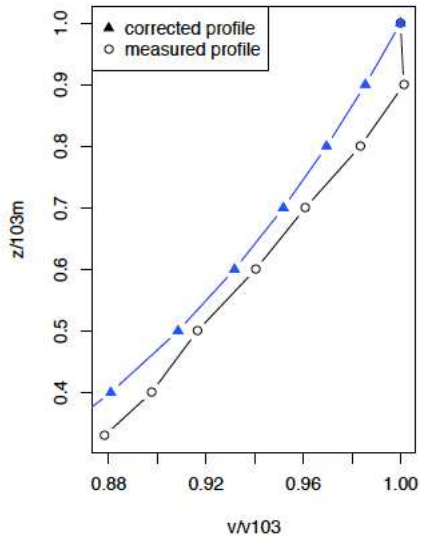

Figure 8.3.1: Measured and corrected wind profile for the period of May-August.

8.4 AEP (P50)

After filtering, long-term prediction and vertical extrapolation were performed, ten-minute wind speed averages at hub height were obtained. The estimation of gross energy (P50) was performed following four successive steps.

In a first step, the probability density p(<u>) for the ten-minute wind speed averages at hub height <u> was used. Random values $\langle u \rangle_{random}$ were drawn from this probability density that represent the ten-minute wind speed average. <u> and $\langle u \rangle_{random}$ have the same distribution (that is close to a Weibull distribution), but $\langle u \rangle_{random}$ is a randomized series.

In a second step, the distribution p(TI) of ten-minute turbulence intensity TI measured at 100 m was considered. No vertical extrapolation to hub height was performed for TI. Similarly to the first step, a randomized series for the turbulence intensity TI_{random} was generated that has the same distribution as TI measured.

In a third step, the randomized series $\langle u \rangle_{random}$ and TI_{random} generated are used. Within each ten-minute interval, a synthetic signal of wind speed u(t) is generated at a sampling frequency of 1Hz following :

$$u(t) = \langle u \rangle_{random}[1 + TI_{random} u'(t)]$$

Where *u'(t)* is a synthetic series with mean value 0 and variance 1 that represents turbulent fluctuations. It is modelled as a simple stochastic process following:

$$du'(t)/dt = - a\, u'(t) + a^{1/2} \,.\, \Gamma(t)$$

With *Γ(t)* a set of Gaussian uncorrelated (random) values with mean value 0 and variance 2. The parameter *a* was extracted from the autocorrelation function $R_{u'u'}(t) \sim exp(-at)$ of the signal *u'(t)* measured for FINO 1 at 100m at 1Hz (additional 1Hz data was used here).

In a fourth step, the synthetic signal of wind speed *u(t)* generated at 1Hz over ten minutes is used. From this 1Hz wind speed signal *u(t)*, a signal of power output *P(t)* is modelled at 1Hz. A stochastic model of Langevin is used following Ref. [8.3] in order to convert *u(t)* into a power signal *P(t)*. In order to perform this model, the power curve is used, as well as typical stochastic parameters estimated for a 2MW wind turbine (additional data was used here). Finally, the ten-minute mean power value is estimated from the 1Hz power signal *P(t)*.

Figure 8.4.1 shows the process.

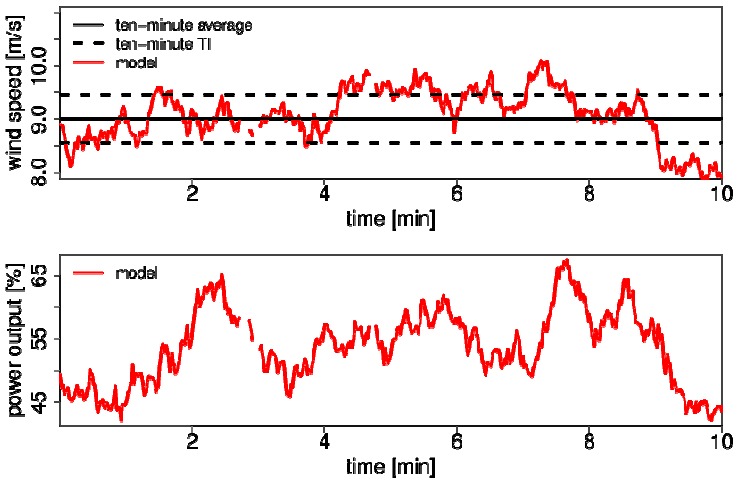

Figure 8.4.1: Example for one ten-minute interval of (upper) 1Hz wind speed u(t) modeled (red line) in the third step using ten-minute average (black line) and ten-minute TI (dashed black line) ; (lower) 1z power output modeled (red line) in the fourth step.

The third and fourth steps are repeated for each ten-minute interval in order to generate ten-minute power output averages over 1 year. These power values are then integrated over 1 year in order to obtain the gross energy production P50. A final value of 9.53GWh is obtained.

8.5 Uncertainty Analysis

Following the procedure in section 8.4, three sources of uncertainty were considered for 10-year estimation.

- A large source of uncertainty comes from the uncertainty in the power curve estimation. We considered an uncertainty of +/-2% for the power values of the power curve, as typically observed in [8.4]. The procedure in section 8.4 was performed three times considering three power curves: the power curve provided, then augmented by +2%, then reduced by -2%. The mean deviation in gross energy considering the changes +2% and -2% was calculated, giving an uncertainty ε_1=0.14GWh (1.49% of P50).
- The energy production P50 is estimated as the sum over ten-minute power samples. When summing up independent values, an estimation of the statistical deviation is given as $\sqrt{N\sigma^2}$, where N is the number of ten-minute intervals over ten years, and σ is the standard deviation of ten-minute power averages. This uncertainty is ε_2=0.09GWh (0.98% of P50).
- Within each ten-minute interval, an average power value is estimated. However, deviations (fluctuations) are observed around this average value. Because the ten-minute intervals are independent from one another, the total uncertainty over 10 years is given as $\sqrt{\sum_i \sigma_i^2}$, where σ_i represents the standard deviation of power output P(t) for ten-minute interval i. This uncertainty is ε_3=0.03GWh (0.31% of P50).

The three independent sources of uncertainty are integrated into the total uncertainty $\varepsilon=(\varepsilon_1^2+\varepsilon_2^2+\varepsilon_3^2)^{1/2}$ =0.17GWh (1.81% of P50).

Finally, an estimation of the P90 value was performed. This value was interpreted as the minimal energy production that should be expected with a probability 90% (only 10% of the possible scenarios would produce less than the P90 value). Considering that scenarios are independent from one another, the value P90 was calculated as the 10% quantile of a Gaussian distribution with mean value P50 and standard deviation ε. A P90 value is found of 9.31GWh (97.68% of P50). This means that there is a probability of 90% to obtain at least 9.31GWh.

9 METHODOLOGY FROM CENER

9.1 Filtering

Data filtering was done with Windograper [9.1] (version 3.1.10) and with in-house software. The filtering process is done in two steps: first typical filters are used to remove erroneous data, and then mast shadowing is considered.

9.1.1 General Filters

The measuring period goes from 13th January 2005 until 30th June 2012. Data have been pre-filtered by DEWI and erroneous measurements are denoted as -999.0.

The total number of data analysed is 392544 ten minutes records.

For the wind speed records the criteria [9.2] used to eliminate data have been:

- Wind speed records equal to zero
- Wind speed standard deviation equal to zero
- Maximum wind speed (gust) < Mean wind speed (10 minutes value)

The criteria used to filtered wind direction have been:

- Wind direction standard deviation equal to zero
- Wind direction standard deviation > 180º
- Wind direction out of range [0º, 360)

According to these criteria the wind speed coverage in all the sensors is similar to the initial coverage and greater than 90% in all the height levels. Wind direction coverage is similar too after this filtering but less than 90% in several levels (80 m, 70 m, 60 m, 50 m and 40 m).

9.1.2 Mast shadowing effect

Wind speed data for all the heights have been plotted versus 90 meters wind direction (only the wind direction for this height has coverage greater than 90%), as one can see in Figure 9.1.1 mean wind speed, except for 100 meters level, present strongly deviating behaviour between 290º and 340º. The reason is the influence of the mast shadow on the anemometers at 90 m, 80 m, 70 m, 60 m, 50 m, 40 m and 33 m, while the top anemometer at 100 meter height does not seem to be affected.

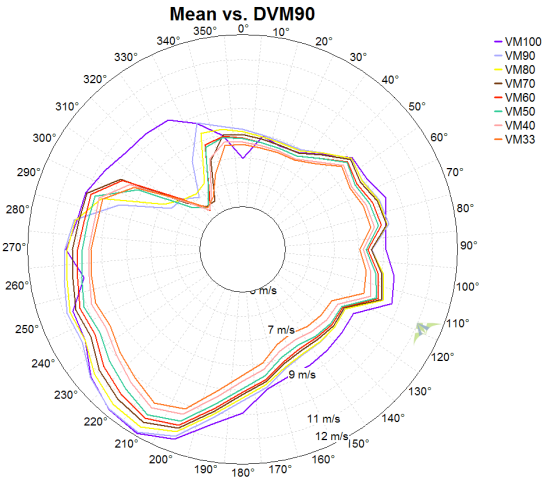

Figure 9.1.1: Mean wind speed distribution of all measured levels versus 90 meters height direction.

To analyze in detail this effect two types of plots are presented, the Figure 9.1.2 shows wind speed measurements from different measurements heights plotted versus each other, on the left; and on the right it shows the ratios of two neighbouring wind speed versus wind direction

For the mean wind speed at 100 m and 90 m height, the scatter plot shows two distinct trends. The stronger one shows the expected ratio of 1:1, while the other reveals a larger slope. It is due to the influence of mast shadow on the anemometer at 90 m height, while the top anemometer at 100 m is unaffected.

The other measurements heights present consistent slopes of 1, with scattering due to mast shadowing. The scattering decreases with decreasing height.

The wind speed ratios for the anemometer at 100 m and 90 m again behave differently. The disturbance of the mast only affects the anemometer at 90 m, but very small disturbances at about 0°, 90°, 180° and 270° wind direction are found, which probably come from the lighting rods on the platform.

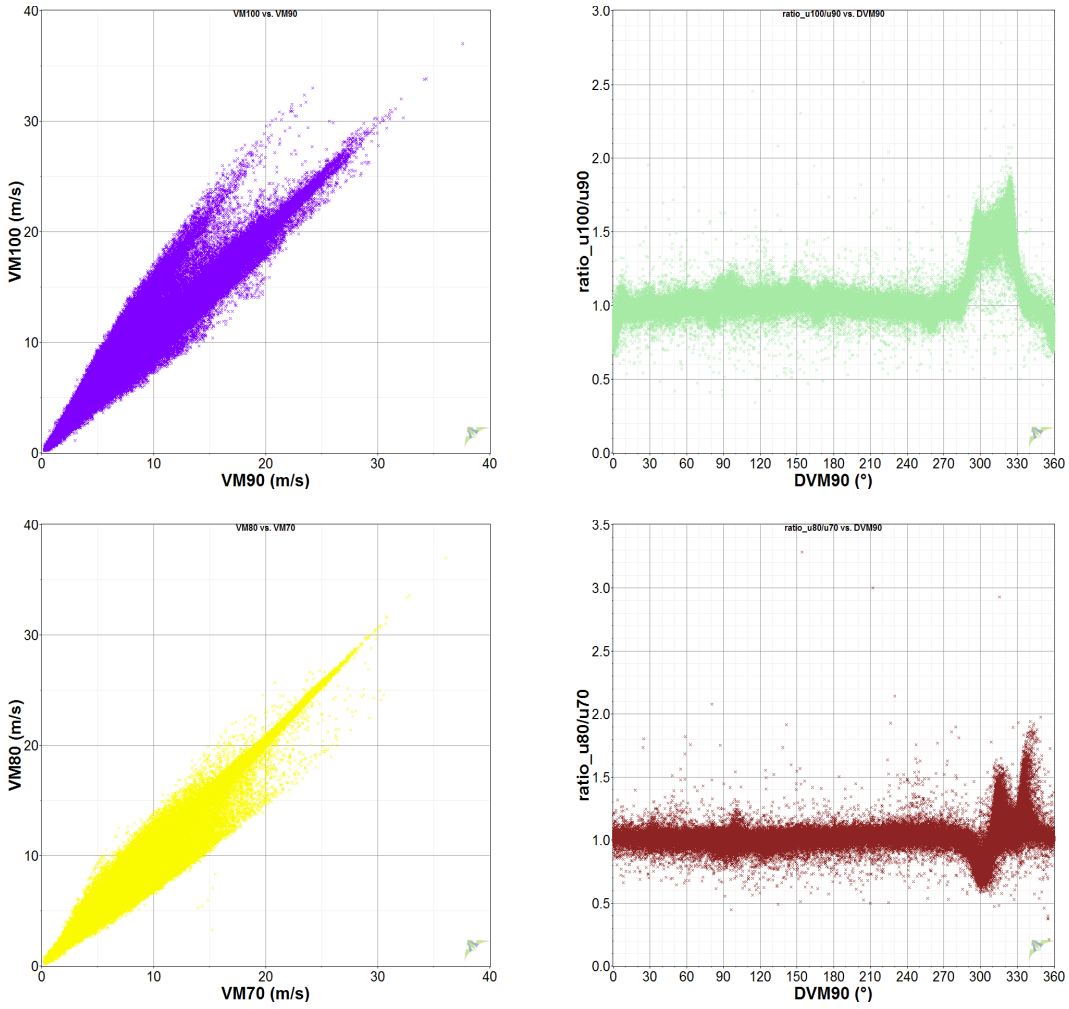

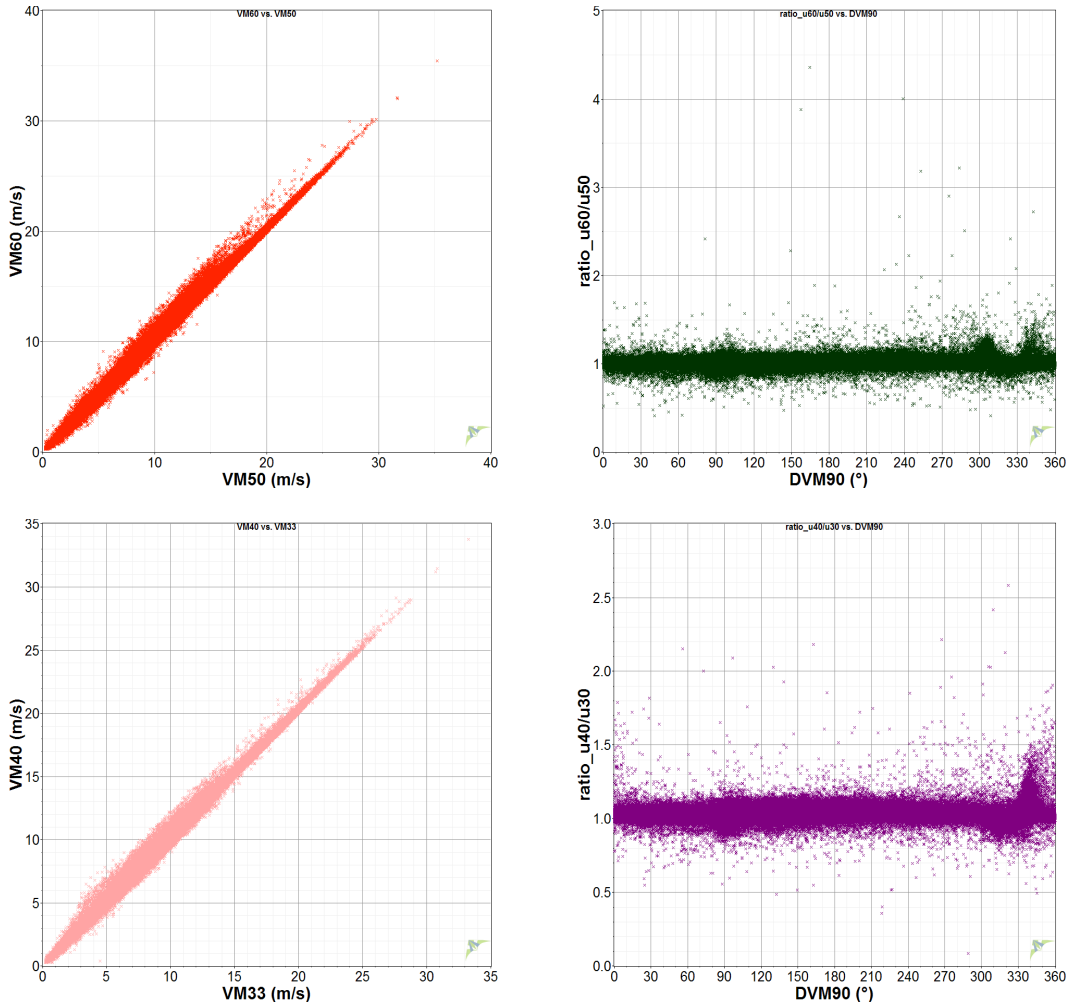

plots are presented, the Figure 9.1.2: On the left wind speed at one height level versus wind speed at lower level. On the right wind speed ratio of cup anemometers at consecutive height level versus the wind direction at 90 meters.

The magnitude of the mast shadow differs for each height, to eliminate perturbed values of wind speed each level has been analyzed and perturbed data (data from 290º to 330º) has been eliminated.

For the FINO 1 data the mast shadow filters have larger effect in the data coverage than general filters with a maximum coverage decreasing by up to 16% for the 33 m wind data.

9.2 Long term

With a measured period covering more than 7 years we would not use any kind of long term correction, unless it comes from a very close and good quality mast with a correlation coefficient larger than 95%. However in order to compare MCP methods and data sources long term correlation analysis has been done with several references.

9.2.1 No long term extrapolation

Assuming that 7 years it is a representative period for the long term conditions in FINO 1 site, the seven-year period has been selected between the total periods (7.5 years), see Table 9.2.1.

Coverage, without eliminate the mast shadowing effect, has been the criterion to select the final reference period: June 2005 to May 2012 with a long term mean wind speed of 9.84 m/s at 100 meters height.

Table 9.2.1: Time periods analyzed with their coverage and 100 m mean wind speed

Time period	Mean wind speed [m/s]	Coverage [%]
Jan2005-Dec2011	9.83	96.12%
Feb2005-Jan2012	9.86	96.31%
Mar2005-Feb2012	9.86	96.24%
Apr2005-Mar2012	9.84	96.61%
May2005-Apr2012	9.82	96.69%
Jun2005-May2012	**9.83**	**96.69%**
Jul2005-Jun2012	9.84	96.68%

9.2.2 With long term extrapolation

Additionally, several reference data sets have been evaluated for long-term extrapolation of the measured wind data; Table 9.2.2 shows their main characteristics.

Table 9.2.2 : Reference data sets and their characteristics

Reference	Spatial resolution	Temporal resolution	Height [m]	Grid point	Time period
Era-Interim reanalysis	1.5°	6 hour	10	54.00°N; 6.75°E	01/01/1979 to 01/01/2012
MERRA[2]	0.50° in latitude and 0.66° in longitude	1 hour	50	54.00°N 6.67°E	24/02/1980 to 01/01/2013
GFS[3]	1.00°	3 hour	10	54.00°N 7.00°E	23/05/2003 to 01/03/2011
Skiron	0.05°	1 hour	100	54.00°N 6.60°E	01/10/2003 to 01/01/2013

[2] MERRA; Modern Era Retrospective-analysis for Research and Applications
[3] GFS; Global Forecast System

Figure 9.2.1 shows the comparison of each of these reference data sets with the FINO 1 measured data. The four sources present good agreement in the wind rose, diurnal wind speed profile and monthly wind speed profile.

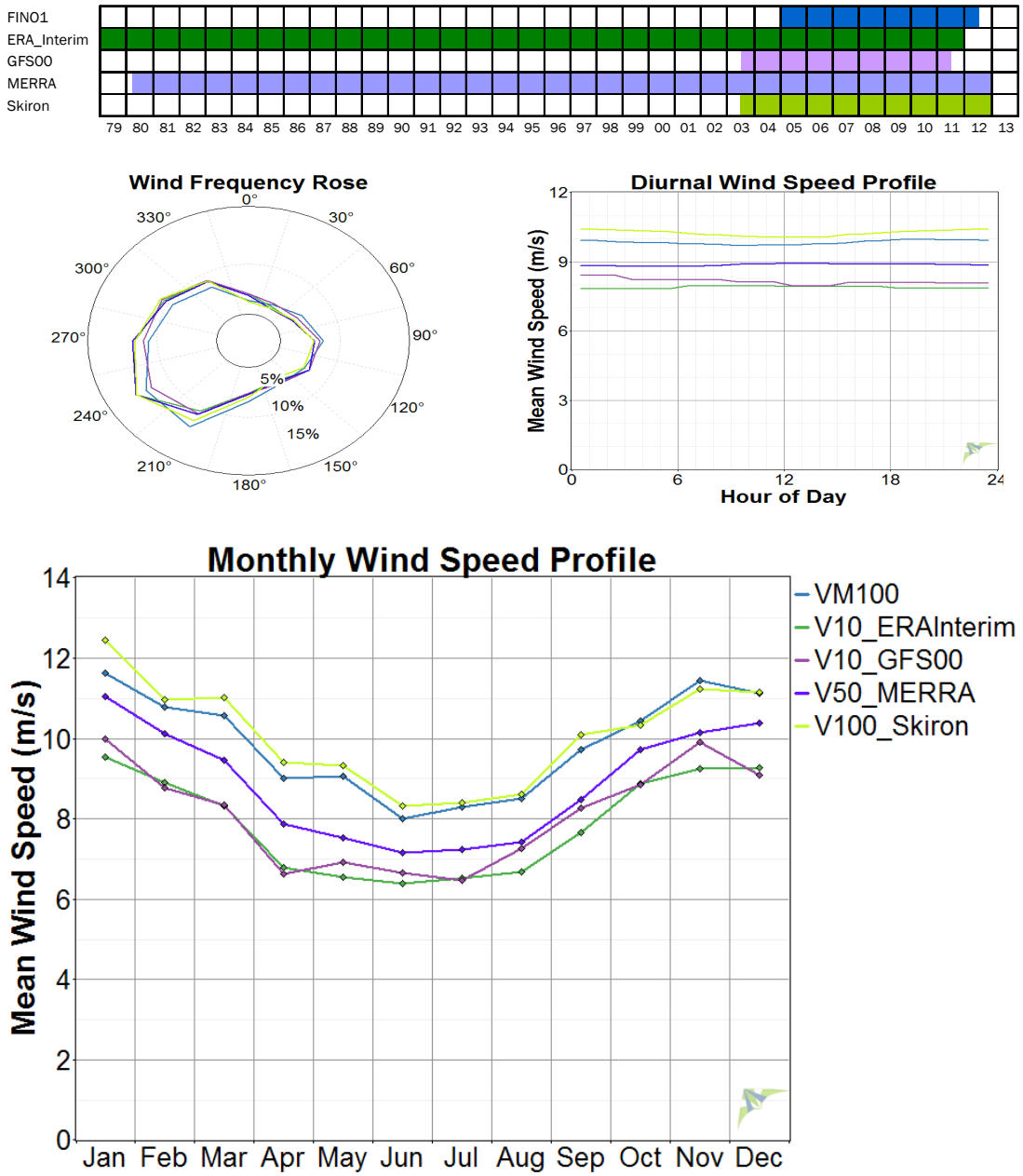

Figure 9.2.1: Comparison between virtual reference data sources and FINO 1 measured data (blue line). Notice that they are referred to different heights as Table 9.2.2

In order to determine the long term mean wind conditions of the site, the FINO 1 measured data was correlated to evaluate the quality of the long term data from the various reference data sets.

For each evaluated long term data source, seven algorithms have been used:

1. Linear Least Squares (LLS)> The classic least squares fit to the scatter plot of target and reference speeds
2. Orthogonal Least Squares (OLS)> A slight modification of LLS that minimizes orthogonal distance to line of best fit
3. Variance Ratio (VR)> A simple linear mapping that aims to preserve the variance of the target data [9.3]
4. Weibull Fit (WBL)> A power law fit whose parameters derive from the Weibull parameters of the target and reference data [9.4]
5. Speed Sort (SS)> A linear fit to the relationship between target and reference cumulative frequency distributions [9.5]
6. Vertical Slice (VS)> A piecewise linear fit to the scatter plot of target and reference speeds [9.6]
7. Matrix Time Series (MTS)> An implementation of the classic matrix method [9.7] that we modified to produce realistic time series data [9.8]

The error statistics have bee calculated in terms of:

- The mean bias error (MBE) is a measure of how closely a set of predicted values match the set of observed or true values. MBE is calculated using the following equation:

$$MBE = \frac{1}{N}\sum_{i=1}^{N}(\hat{y}_i - y_i)$$

Where *N* is the number of values in the set, *yi* is the i[th] observed value and $\hat{y}_i$ is the i[th] predicted value. The MBE is equal to the mean of the predicted values minus the mean of the observed values. It measures the mean bias in the predictions.

- The mean absolute error (MAE) is a measure of how closely a set of predicted values match the set of observed or true values. MAE is calculated using the following equation:

$$MAE = \frac{1}{N}\sum_{i=1}^{N}|\hat{y}_i - y_i|$$

Where *N* is the number of values in the set, *yi* is the i[th] observed value and $\hat{y}_i$ is the i[th] predicted value.

- The root mean squared error (RMSE) is a measure of how closely a set of predicted values match the set of observed or true values. RMSE is calculated using the following equation:

$$RMSE = \frac{1}{N}\sqrt{\sum_{i=1}^{N}(\hat{y}_i - y_i)}$$

Where *N* is the number of values in the set, *yi* is the i[th] observed value and $\hat{y}_i$ is the i[th] predicted value.

- The distribution error (DE) is a measure of how closely the distribution of a set of predicted values matches the distribution of the observed or true values. To calculate the distribution error, two frequency distributions are constructed; one for the predicted values and one for the observed values, making sure the two distributions have the same number and size of bins. Then it computes the DE as the Pearson's chi-squared test statistic, using the following equation:

$$DE = \sum_{i=1}^{N}\frac{(\hat{F} - F_{ii})^2}{F_i}$$

Where *N* is the number of values in the set, *Fi* is the i[th] observed value and $\hat{F}_i$ is the i[th] predicted value.

Each of these methods has been tested for only 1 sector and for 16 sectors.

The results obtained have been:

- **Era Interim**> The long term period is extended from 7 years to 33 years and the best fit in this case is the Linear Least Squares, the results are quiet similar either using one sector or sixteen sectors. Table 9.2.3 and Table 9.2.4 present these results. A time offset of 3 hours has been applied to the reference data.

Table 9.2.3: Mean Bias Error, Mean Absolute Error, Root Mean Squared Error, Distribution error and R^2 for FINO 1 correlated with Era Interim data (1 sector)

Metric	LLS	OLS	VR	WBL	SS	VS	MTS
MBE (m/s)	0.22	0.24	0.23	0.25	0.22	0.22	0.27
MAE (m/s)	1.59	1.65	1.62	1.63	1.63	1.59	2.15
RMSE (m/s)	2.01	2.11	2.07	2.07	2.08	2.01	2.72
Distribution error (%)	4.39	12.00	3.80	4.72	4.79	8.88	1.38
R^2	0.78	0.76	0.77	0.77	0.77	0.78	-

Table 9.2.4: Mean Bias Error, Mean Absolute Error, Root Mean Squared Error, Distribution error and R^2 for FINO 1 correlated with Era Interim data (16 sectors)

Metric	LLS	OLS	VR	WBL	SS	VS	MTS
MBE (m/s)	0.24	0.28	0.27	0.29	0.24	0.24	0.29
MAE (m/s)	1.60	1.72	1.67	1.67	1.69	1.61	2.17
RMSE (m/s)	2.04	2.21	2.15	2.15	2.16	2.05	2.77
Distribution error (%)	3.65	20.70	8.24	5.49	6.57	6.60	1.17
R^2	0.77	0.75	0.76	0.76	0.75	0.79	-

- **MERRA>** The long term period is extended from 7 years to 32 years and the best fit in this case is the Linear Least Squares, the results are quiet similar either one sector or sixteen sectors. Table 9.2.5 and Table 9.2.6 present these results.

Table 9.2.5: Mean Bias Error, Mean Absolute Error, Root Mean Squared Error, Distribution error and R^2 for FINO 1 correlated with MERRA data (1 sector)

Metric	LLS	OLS	VR	WBL	SS	VS	MTS
MBE (m/s)	0.20	0.19	0.19	0.20	0.20	0.20	0.22
MAE (m/s)	1.23	1.24	1.24	1.24	1.24	1.25	1.59
RMSE (m/s)	1.62	1.64	1.64	1.63	1.63	1.62	2.05
Distribution error (%)	2.12	1.05	0.95	0.75	0.70	5.76	1.23
R^2	0.87	0.87	0.87	0.87	0.87	0.87	-

Table 9.2.6: Mean Bias Error, Mean Absolute Error, Root Mean Squared Error, Distribution error and R^2 for FINO 1 correlated with MERRA data (16 sectors)

Metric	LLS	OLS	VR	WBL	SS	VS	MTS
MBE (m/s)	0.21	0.22	0.22	0.22	0.22	0.21	0.17
MAE (m/s)	1.25	1.30	1.28	1.28	1.28	1.25	1.57
RMSE (m/s)	1.65	1.73	1.71	1.70	1.71	1.65	2.05
Distribution error (%)	1.59	1.71	1.23	0.71	0.60	4.54	1.11
R^2	0.86	0.85	0.85	0.86	0.85	0.80	-

- **GFS>** The long term period is extended from 7 years to 9 years and the best fit in this case is the Linear Least Squares, the results are quiet similar either one sector or sixteen sectors. Table 9.2.7 and Table 9.2.8 present these results. A time offset of 2 hours has been applied to the reference data.

Table 9.2.7: Mean Bias Error, Mean Absolute Error, Root Mean Squared Error, Distribution error and R^2 for FINO 1 correlated with GFS data (1 sector)

Metric	LLS	OLS	VR	WBL	SS	VS	MTS
MBE (m/s)	0.25	0.25	0.25	0.26	0.25	0.22	0.18
MAE (m/s)	1.53	1.59	1.57	1.56	1.57	1.54	2.06
RMSE (m/s)	1.98	2.06	2.03	2.03	2.04	1.97	2.65
Distribution error (%)	5.56	3.53	2.36	2.53	2.57	9.45	1.00
R^2	0.79	0.78	0.78	0.78	0.78	0.79	-

Table 9.2.8: Mean Bias Error, Mean Absolute Error, Root Mean Squared Error, Distribution error and R^2 for FINO 1 correlated with GFS data (16 sectors)

Metric	LLS	OLS	VR	WBL	SS	VS	MTS
MBE (m/s)	0.28	0.31	0.30	0.31	0.29	0.25	0.22
MAE (m/s)	1.52	1.62	1.59	1.58	1.59	1.53	2.04
RMSE (m/s)	1.97	2.11	2.06	2.06	2.07	1.98	2.63
Distribution error (%)	4.84	4.13	2.04	2.41	2.62	6.94	0.70
R^2	0.79	0.77	0.77	0.77	0.77	0.75	-

- **Skiron data set**> The long term period is extended from 7 years to 9 years and the best fit in this case is the Linear Least Squares method, the results are quiet similar either one sector or sixteen sectors. Table 9.2.9 and Table 9.2.10 present these results. A time offset of 1 hour has been applied to the reference data.

Table 9.2.9: Mean Bias Error, Mean Absolute Error, Root Mean Squared Error, Distribution error and R^2 for FINO 1 correlated with SKIRON data (1 sector)

Metric	LLS	OLS	VR	WBL	SS	VS	MTS
MBE (m/s)	0.31	0.30	0.30	0.31	0.30	0.30	0.32
MAE (m/s)	1.54	1.56	1.56	1.56	1.57	1.55	1.96
RMSE (m/s)	2.06	2.12	2.13	2.13	2.13	2.06	2.55
Distribution error (%)	3.51	0.34	0.34	0.44	0.52	8.25	0.92
R^2	0.80	0.78	0.78	0.78	0.78	0.80	-

Table 9.2.10: Mean Bias Error, Mean Absolute Error, Root Mean Squared Error, Distribution error and R^2 for FINO 1 correlated with SKIRON data (16 sectors)

Metric	LLS	OLS	VR	WBL	SS	VS	MTS
MBE (m/s)	0.29	0.30	0.30	0.31	0.29	0.29	0.25
MAE (m/s)	1.53	1.55	1.56	1.56	1.56	1.54	1.98
RMSE (m/s)	2.05	2.11	2.12	2.12	2.12	2.05	2.58
Distribution error (%)	3.70	0.35	0.33	0.42	0.47	7.97	1.14
R^2	0.78	0.77	0.76	0.76	0.76	0.65	-

Taking into account the results, the reference data selected for long-term correlation with the measured wind data has been based on MERRA database.

The long term period obtained is January 1981 to December 2012 with a long term mean wind speed of 9.91 m/s at 100 meters height, 0.7% higher than the seven years measured wind speed.

9.3 Vertical extrapolation

Vertical extrapolation allows extrapolating upwards from the heights at which there are measured wind speed data to estimate the wind speeds typically at hub-height.

There are several theoretical expressions used for determining the wind speed profile [9.9]. The Monin-Obukhov theory is often used for the description of the mean wind speed profile over flat terrain. From a given wind speed at one given height, the profile is predicted using the two parameters Monin-Obukhov length and sea surface roughness:

$$U(z) = \frac{u_f}{K}\left[\ln\frac{z}{z_0} - \Psi\left(\frac{z}{L}\right)\right]$$

Where U is the wind speed, z is the height above ground level, u_* is the friction velocity, κ is the von Karman constant (normally assumed as 0.4), z_0 is the surface roughness length, $\Psi(z/L)$ is the stability function and L is a scale factor called the Monin-Obukhov length. This equation is strictly valid only for quasi-steady conditions in the surface layer although it can also provide good predictions of ensemble-averaged atmospheric boundary layer profiles in sites with predominant unstable-neutral conditions.

This equation has been proven satisfactory for detailed surveys at critical sites; however, such a method is difficult to be applied for general engineering studies. Thus the surveys must resort to simpler expressions and secure satisfactory results even when they are not theoretically accurate [9.10]. The most commonly used of these simpler expressions is the Hellmann exponential law that correlates the wind speed readings at two different heights and is expressed by:

$$\frac{U_2}{U_1} = \left(\frac{z_2}{z_1}\right)^{\alpha}$$

Where α is the Hellman exponent (sometimes called shear exponent, power law coefficient, friction coefficient or simply 'alpha') determined by the velocity at two levels. The coefficient varies with the height, hour of the day, time of the year, land features, wind speeds and temperature.

Another formula, the Monin-Obukhov for neutral stability, known as the logarithmic wind profile law and which is widely used is the following:

$$U(z) = \frac{u_f}{K}\ln\frac{z}{z_0}$$

Where z is height, u_f is the friction velocity, K is the von Karman constant (normally assumed as 0.4) and z_0 is called the roughness coefficient length is expressed in meters and depends basically on the land type, spacing and height of the roughness factor (water, grass, etc.) and it ranges from 0.0002 up to 1.6 or more [9.11].

To estimate the mean wind speed at hub height (120 m) in FINO 1 Hellmann exponent law and logarithmic wind profile law have been used.

9.3.1 Hellmann exponential law

For FINO 1 filtered data sets (sectors, in which the mast disturbed the incoming wind flow of the sensor were filtered out) containing wind speeds at 33, 40, 50, 60, 70, 80, 90 and 100 meters above ground, the power law exponent that best fits the vertical wind speed profile has been calculated, see Figure 9.3.1. The calculation has been performed for each time step.

A mean height exponent of α=0.101 was determined by the measurements of the different heights, and this has been used to extrapolate wind speed to hub height.

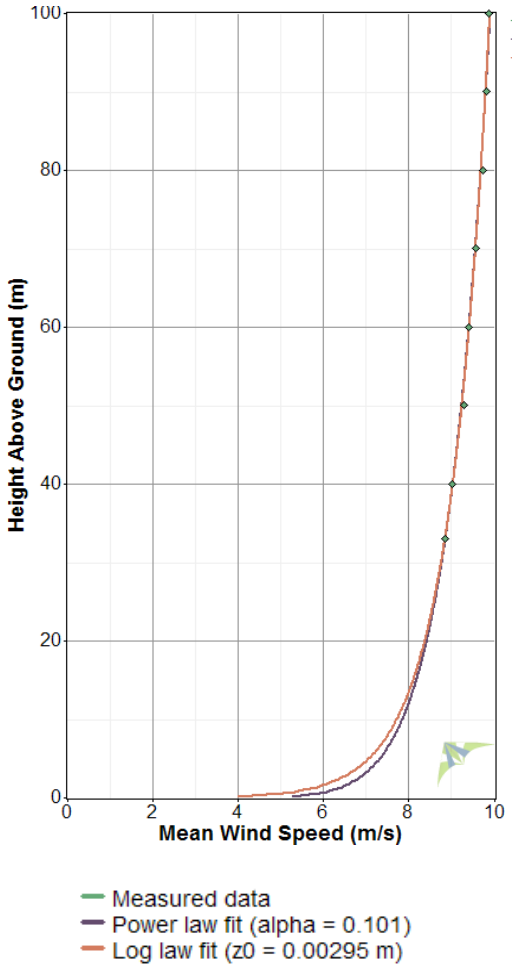

Figure 9.3.1: Wind profile built up using the Hellman law and logarithmic law for FINO 1

To validate the methodology the same analysis has been done without using the 100 m level and extrapolating the results from 90 m to 100 m. A height exponent of α=0.103 was determined and a deviation of 0.47% between measured and extrapolated 100 meters wind speed has obtained. The error is within measurement uncertainty, not surprising given the short extrapolation.

Power law exponent has been analyzed versus wind direction sector, month and time of day, see Figure 9.3.2. Power law exponent has variations along the hour of the day and larger variations along the months.

The power-law exponent is an indirect indicator of atmospheric stability: the larger the magnitude of the exponent the more stable. Neutral and unstable conditions present lower power-law exponents as a result of a much higher turbulence mixing. The diurnal variability is more important in the months from March to July when air-sea temperature differences have larger diurnal variability. On a monthly basis, larger exponents are found in the months of March-May, when the frequency of stable conditions is larger. The contrary happens in the months of October-December where more unstable conditions happens which results in flatter profiles.

The rose of shear exponent shows that larger exponents are found in the sectors where the coast is the nearest. This is due to the higher frequency of situations where warm air from the coast is advected over colder water, producing a stable boundary layer which results in larger wind shear.

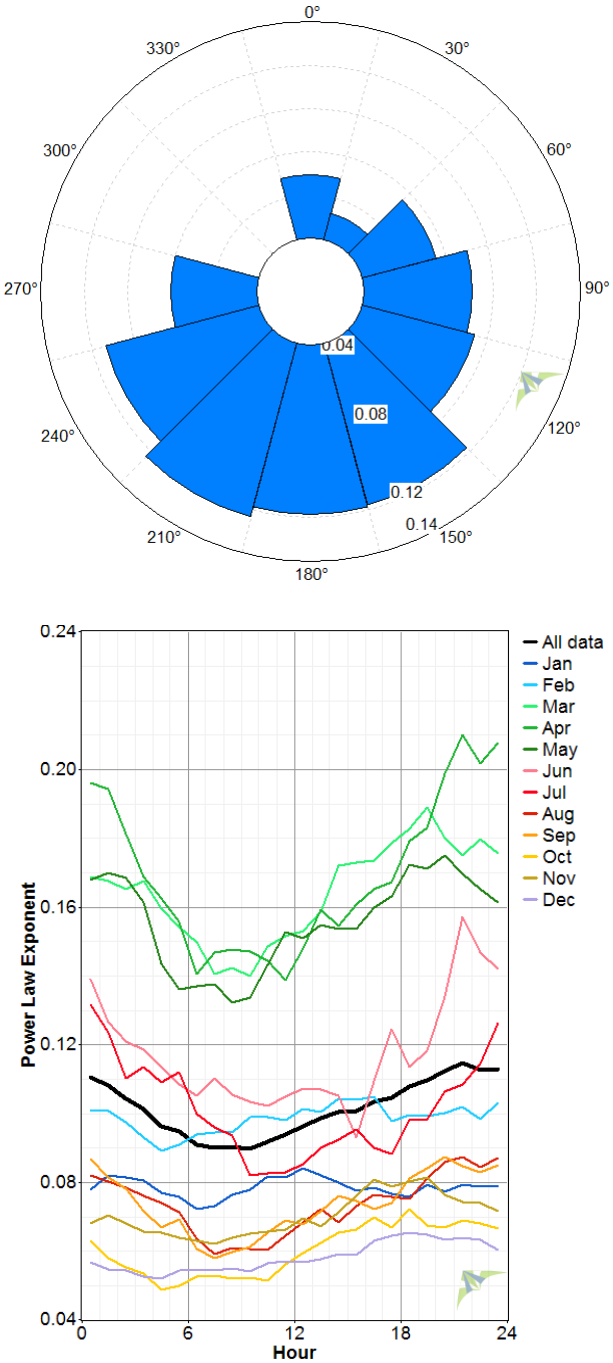

Figure 9.3.2: Power law exponent versus direction, month and time of day.

9.3.2 Logarithmic wind profile law

The surface roughness value that best fit the measured vertical wind speed profile assuming neutral conditions in the log-law is 0.0029 m, see Figure 9.3.1. It has been calculate in each time step and averaged.

This value is little bit higher than the standard value used for offshore sites (0.0002 m) in engineering models

To validate the methodology, the same analysis has been done without using the 100 m level and extrapolating the results from 90 m to 100 m. A Surface roughness of z_0=0.0031 was determined and a deviation of 0.13% between measured and extrapolated 100 meters wind speed has obtained.

Surface roughness has been analyzed versus wind direction sector, month and time of day, see Figure 9.3.3. Surface roughness has variations along the hour of the day and larger variations along the months.

The behavior of the power law exponent and surface roughness versus sector direction month and time of day is the same. Similarly to the power-law method, since stability correction has not been considered in the log-law, the roughness length after fitting is sensitive to the presence of stability. Logarithmic wind profile law gives better results for this case of FINO 1.

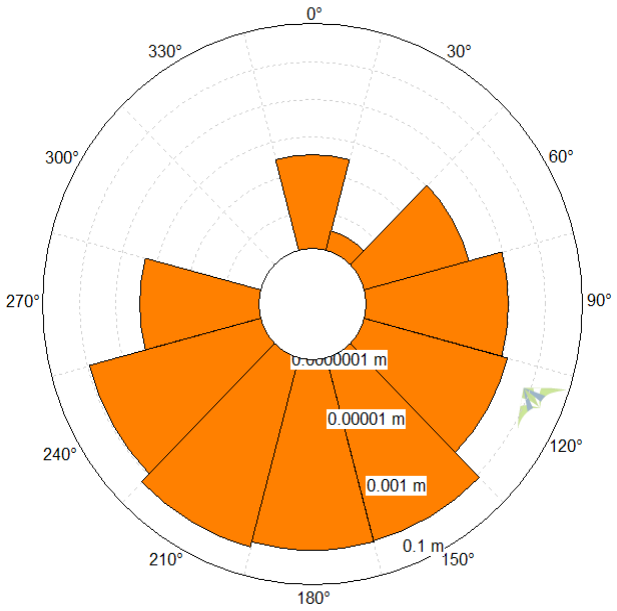

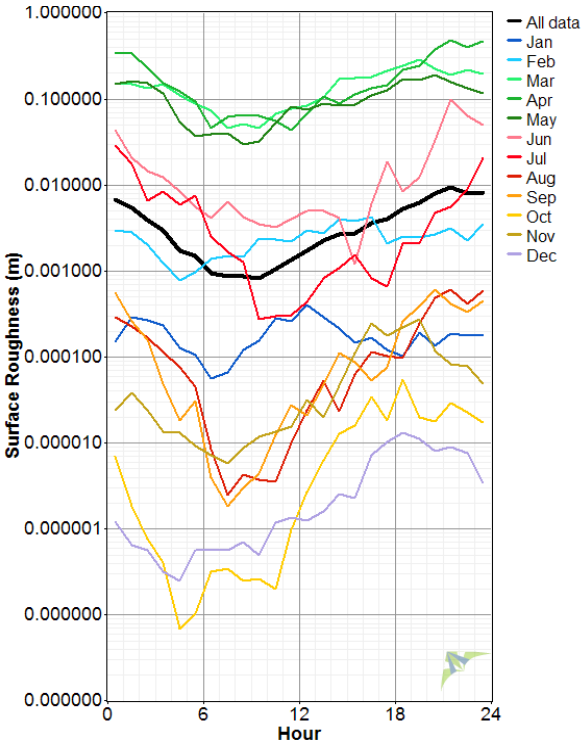

Figure 9.3.3: Surface roughness versus direction, month and time of day.

9.4 AEP (P50)

The gross energy (before accounting for losses) depends on three factors: the turbine's power curve, the wind speed at hub height, and the air density.

Once the appropriate power curve has been chosen, the power output is calculated by referring to the power curve and performing an air density correction to account for any difference between the actual air density and the air density at which the power curve applies. This air density correction is performed according to the recommendations of IEC standard 61400-12 (2005) [8.4]. The nature of this air density correction depends on the power regulation method that the wind turbine uses.

In this case a power curve for 1.225 kg/m^3 air density has been used and no air density correction has been done as it was predefined in the method intercomparison study.

The annual gross energy has been obtained according to:

$$E_a = \sum_i P(U_i) T_i$$

Where $P(U_i)$ is the power output for each wind speed interval i and T_i the number of hours in a year for each wind speed interval ($T_i = f_i * 8760$, with f_i the frequency of each wind speed interval).

9.5 Uncertainty Analysis

For the estimation of the average wind speed at FINO 1 used for the estimation of the long-term wind conditions transferred to hub height (120 meters), the next uncertainty components have been quantified:

- Associated to the anemometer and instrumentation system [9.12], the main uncertainty sources are:

  - Calibration of anemometer.
  - Possible variations or changes over the calibration.
  - Possible overestimations on registered speeds caused by instruments dynamics.
  - Flow inclination effects at calibration.
  - Mast flow distortion.
  - Booms flow distortion.
  - Flow distortion due to supporting device.
  - Asymmetry of incident flow at the anemometer.
  - Uncertainties from acquisition system, including calibration and quantifying effects.
- Associated to temporal extrapolation, this uncertainty is associated to the correlation between the FINO 1 mast and the reference mast.
- Associated to vertical extrapolation.
- Associated to the variability of the reference period [9.13].
- Associated to the future variability of the long-term mean velocity. This uncertainty is estimated at 6.1% for a one-year period and 1.9% for a 10-year period.

To translate this wind speed uncertainties to energy uncertainties the wind speed sensitivity factor, the change in energy production for a unitary change in wind speed, has been calculated.

Besides the above mentioned uncertainties, there is also uncertainty associated to the power curve. It has been assumed with a standard value of 5%.

The overall uncertainty is assessed by a combination of its individual components. These are considered independent from each other so the combined standard uncertainty is the square root of the summed squares of the uncertainty components.

10 FINO 1 VIRTUAL MAST (CENER)

CENER uses Skiron for numerical weather prediction (NWP) at mesoscale level. Skiron was developed for operational use by the Hellenic National Meteorological Service and it is supported by the University of Athens. The model is based on the Eta limited area weather forecasting model based on finite differences over a semi-staggered E grid. CENER uses Global Forecasting System (GFS, from NCAR/NCEP) as forcing database to initialize the model daily at 12 UTC. The horizontal resolution is 0.05ºx0.05º latitude/longitude and simulates 50 Eta vertical levels with a time step of 15 seconds to yield hourly forecasts for a 51 hours prediction. The model simulates a single domain that captures the dominant synoptic patterns of the region of interest without nesting. Turbulence is parameterized [10.1] with 2.5-order scheme with Monin-Obukhov similarity theory imposed at the surface layer based on stability functions [10.2].

A period of ten years (June 2003-May 2013) has been simulated in order to produce a long-term database valid for wind atlas mapping, virtual masts and spatial planning operations. The domain that captures the dominant synoptic patterns of the region of interest without nesting is shown in Figure 10.1.

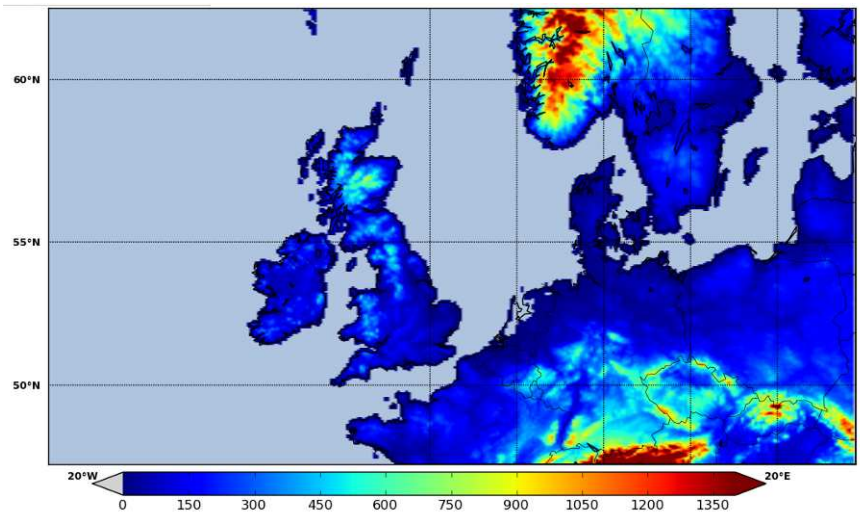

Figure 10.1: Skiron domain with elevation contours in meters to the North Sea region (0.05x0.05 degrees resolution)

To analyze the mesoscale outputs as offshore virtual masts the gross annual energy production has been calculated with data from FINO 1 nearest grid point of Skiron mesoscale model (54.00ºN, 6.60ºE); Figure 10.2 shows the diurnal wind speed profile, vertical wind shear profile, monthly wind speed profile and wind rose obtained from seven years hourly measured and modelled data. The first four Skiron Eta levels are at the next heights above ground level:

- Eta 1 at 9.99 m
- Eta 2 at 34.03 m
- Eta 3 at 68.60 m
- Eta4 at 116.47 m

Comparison with the measured data shows high quality predictions of the model.

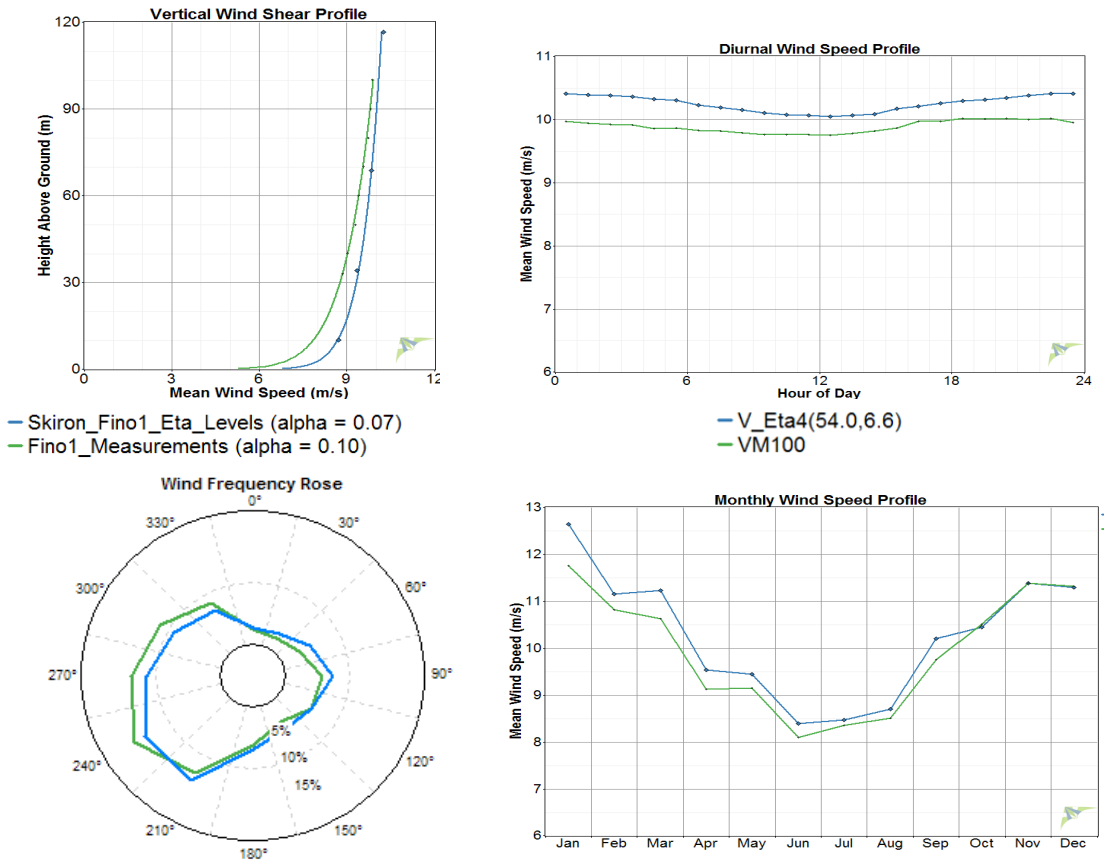

Figure 10.2: Seven years of measured (green line) and modeled (blue line) wind flow characteristics from FINO1. For the vertical profile four eta levels from Skiron have been compared with measurements. Mean wind speed at Eta 4 level has been compared with 100 m measured wind speed in the diurnal wind speed and monthly wind speed

Ten years of hourly wind speed and direction at 120 meters height have been used to estimate the gross energy at FINO 1 site.

Gross energy estimation with mesoscale outputs avoid the data filtering (general quality check for each simulation is done) and the vertical extrapolation. Instead vertical interpolation is done from the levels next to the ground. Long term correlation is not mandatory because 10 years of simulation are considered representative for the long time [10.3].

The uncertainties associated to the measurement and the vertical extrapolation both are replaced by the model uncertainty.

11 RESULTS

With FINO 1 measured data at different height levels and a power curve as input CIEMAT, CRES, RES, Forwind and CENER have estimated the Gross Annual Energy production.

CENER presents different results, in some steps, obtained by the use of different approaches.

The analyzed results are, the recovery rate and mean wind speed after filtering, the long term mean wind speed, the mean wind speed at hub height, the gross energy (P50) the uncertainties considered and the gross energy (P90).

A summary of the submitted results is given in Table 11.1. CV is the coefficient of variation.

Table 11.1: Summary of the results. Recovery rate and mean wind speed only for 100 m level.

Topic	Unit	Mean	σ	Max.	Min.	CV [%]
Recovery rate	%	89.43	9.99	96.55	72.22	11.17
V filtered	m/s	9.88	0.05	9.95	9.84	0.47
LT V	m/s	9.92	0.07	10.03	9.84	0.74
Hub V	m/s	10.08	0.07	10.18	10.02	0.67
TI measured	%	6.35	0.30	6.54	5.82	4.77
LT TI	%	6.38	0.20	6.54	6.05	3.08
Hub TI	%	6.23	0.27	6.47	5.82	4.36
Gross Energy (P50)	GWh	10.00	0.39	10.64	9.46	3.89
Uncertainty	%	5.04	1.91	6.90	1.81	38.00
Gross Energy (P90)	GWh	9.38	0.39	10.14	9.06	4.16

Detailed results of each step are shown in the next points in plots where the y-axis corresponds to the mean value of the submitted results ± deviation. The x-axis shows the number of each team, if no number is given, the result has not submitted by the team.

11.1 Filtering

To check the different filtering criterion used by the companies and their impact in the data set, mean wind speed, wind speed distribution and data recovery rate after filtering has been analyzed.

Figure 11.1.1 shows the deviations from the mean value between participants in the recovery rate after filtering in the 100 m level; it is observed large deviations in this value. These deviations are lower in the top anemometer than in the others heights levels with the largest deviations in the 60 m height level, see Figure 11.1.2.

This deviations are mainly due to the mast shadow influence and how the filtering of the measurements was performed by each participant, since some participants have eliminated the data affected by this effect (participants 2, 3, 4 and 6) but others have not (participants 1 and 5).

In the case of participant 4 they have filtered only the time period of FINO 1 data without wind farm influence (13 of January 2005 to 14 of July 2009) so the period analyzed by them is different from the others.

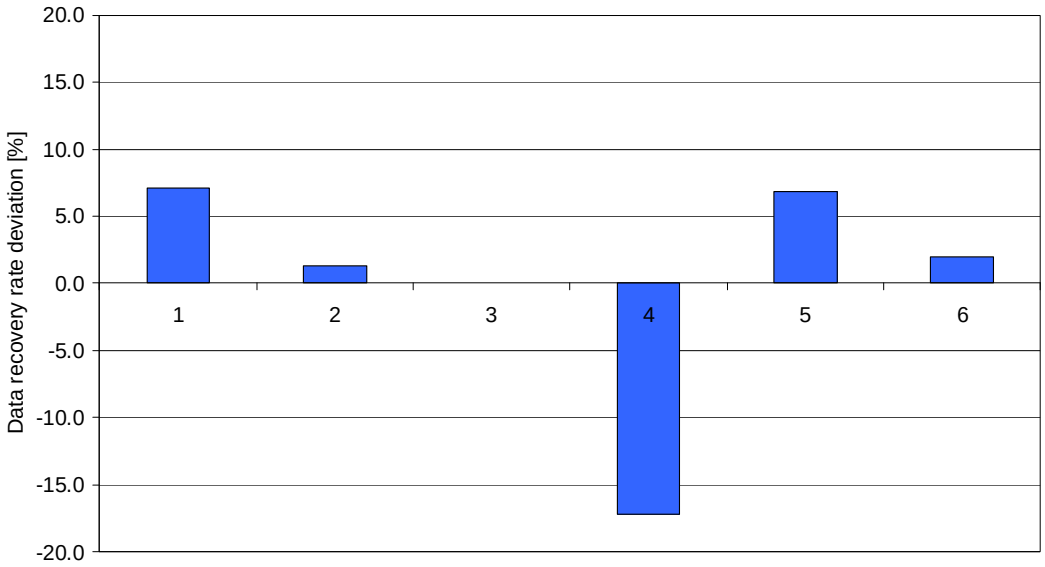

Figure 11.1.1: Recovery rate after filtering in the 100 m height level

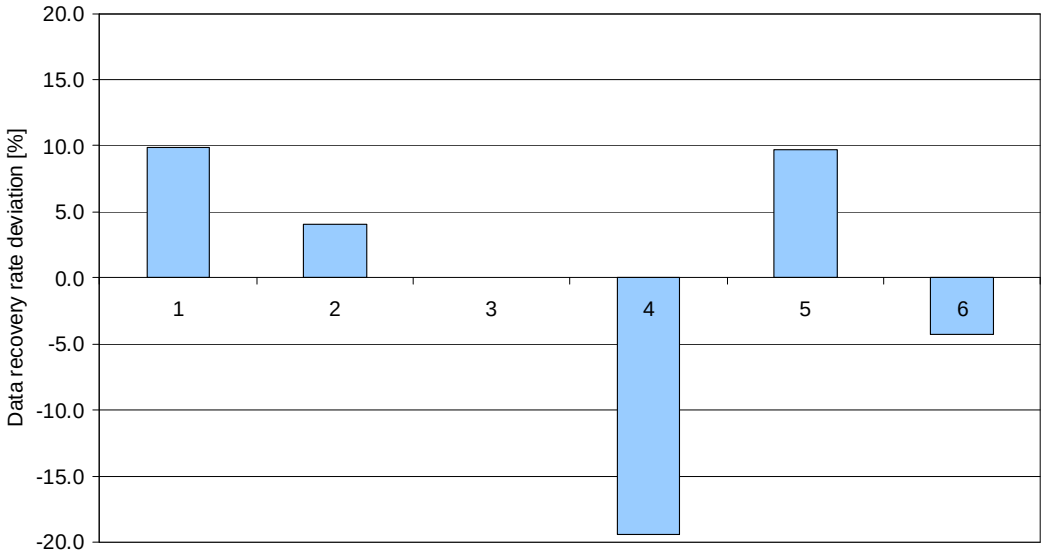

Figure 11.1.2: Recovery rate after filtering in the 60 m height level

The influence in the mean wind speed of the filtering process has been analyzed comparing the mean wind speed, obtained by averaging every 10 minutes wind speeds, for the period considered (see Figure 11.1.3) with the mean wind speed obtained from frequency distribution of hours in the year as a function of wind speed and direction for the 100 meters level (see Figure 11.1.4).

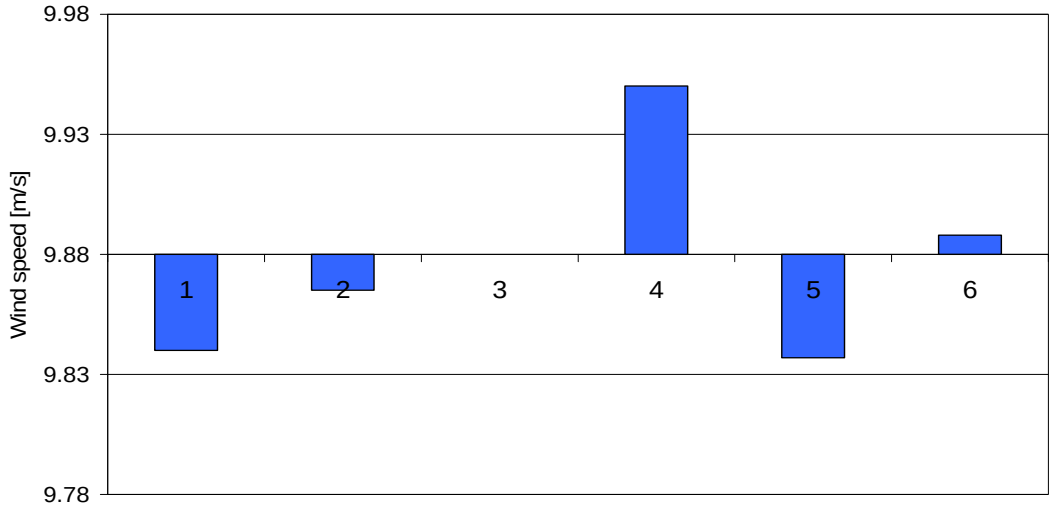

Figure 11.1.3: Mean wind speed after filtering at 100 m obtained as mean of ten minutes value. Mean value ± 1.0%

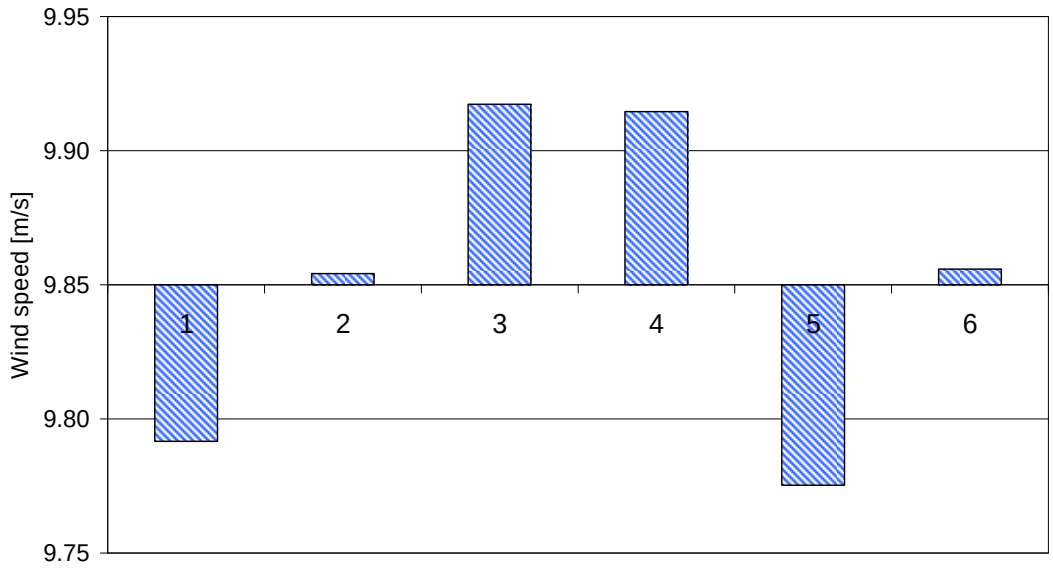

Figure 11.1.4: Mean wind speed after filtering at 100 m obtained from frequency distribution of hours in the year as a function of wind speed and direction. Mean value ± 1.0%

The influence of the filtering in the mean wind speed is smaller than expected at least at the top height anemometer. Figure 11.1.4 shows higher deviations in the mean wind speed than Figure

11.1.3 because the wind direction filtering also affects the mean wind speed derived from frequency distributions.

Figure 11.1.5 shows the frequency wind speed distribution at 100 meter and Figure 11.1.6 the frequency wind rose for 100 m wind speed taking into account the 90 m wind direction. Some higher deviation in the wind rose is appreciated for participant 4.

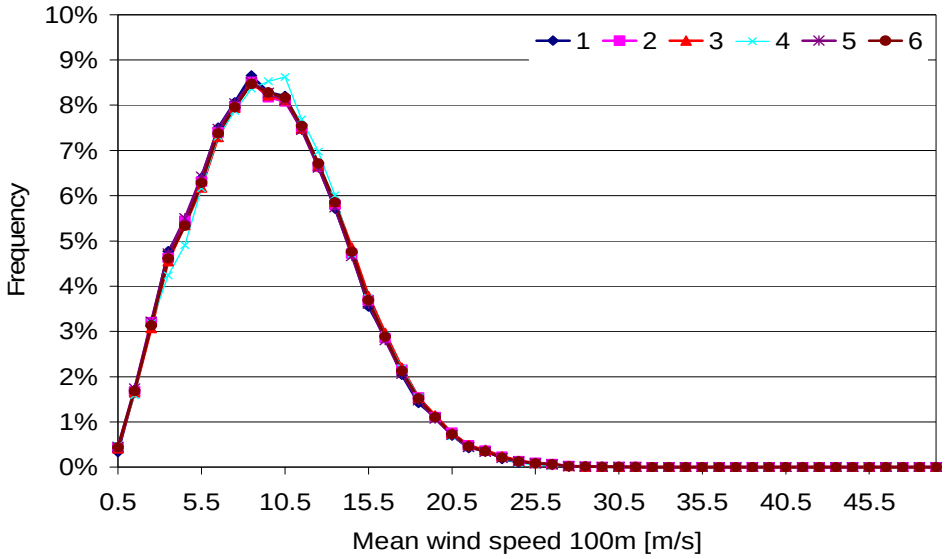

Figure 11.1.5: Wind speed frequency distribution at 100 m height level

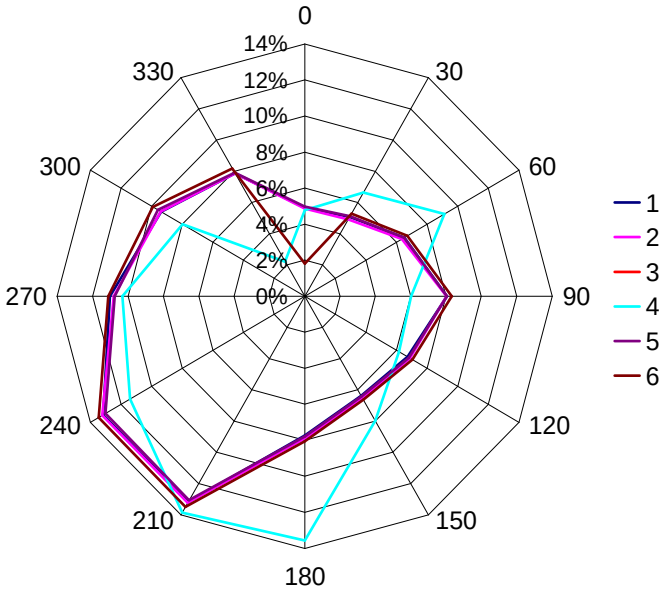

Figure 11.1.6: Frequency wind rose

11.2 Long term

The next step considered in FINO 1 test case is the long term extrapolation. For this step the data reference, the long term period and the correlation method followed have been a free decision for each participant.

Table 11.2 summarizes all the methodologies employed.

Table 11.2: Summary of long term period, data reference a method employed in Long term extrapolation.

Participant	Long term period	Long term method
1	From Jan 2005 to Dec 2011	No long term correction
2	From Jan 1983 to Dec 2012	Long-term correction based on monthly NCAR data.
3	From Jan 1996 to Jun 2012	Long-term correction based hourly MERRA data as the reference source. A matrix correlation method was used.
4	From Jan 1979 to Dec 2011	Long-term correction based on monthly reanalysis data. The MCP method was applied for 12 different directional sectors.
5	From Jun 2005 to May 2012	No reference.
6	From Jan 1981 to Dec 2012	Long-term correction based hourly MERRA data as the reference source. A lineal correlation method was used.

In spite of the different long term methods, references and periods used the 100 m long term mean wind speed obtained has variations lower than 1.5%, see Figure 11.2.1.

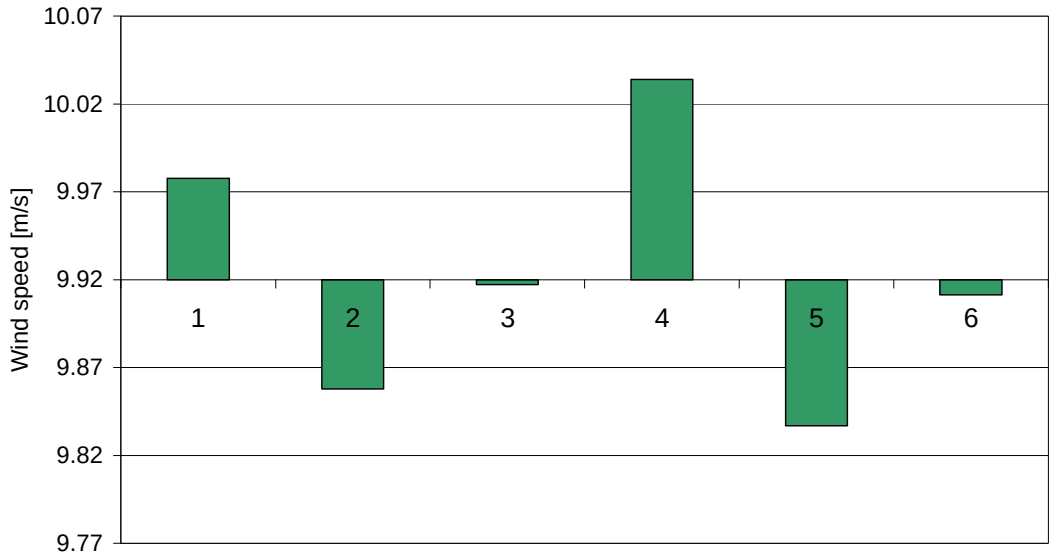

Figure 11.2.1: Long term mean wind speed at 100 m obtained from frequency distribution of hours in the year as a function of wind speed and direction. Mean value ± 1.5%

Analyzing the frequency wind speed distribution, see Figure 11.2.2, the deviations are higher than in the results obtained after filtering (Figure 11.1.5).

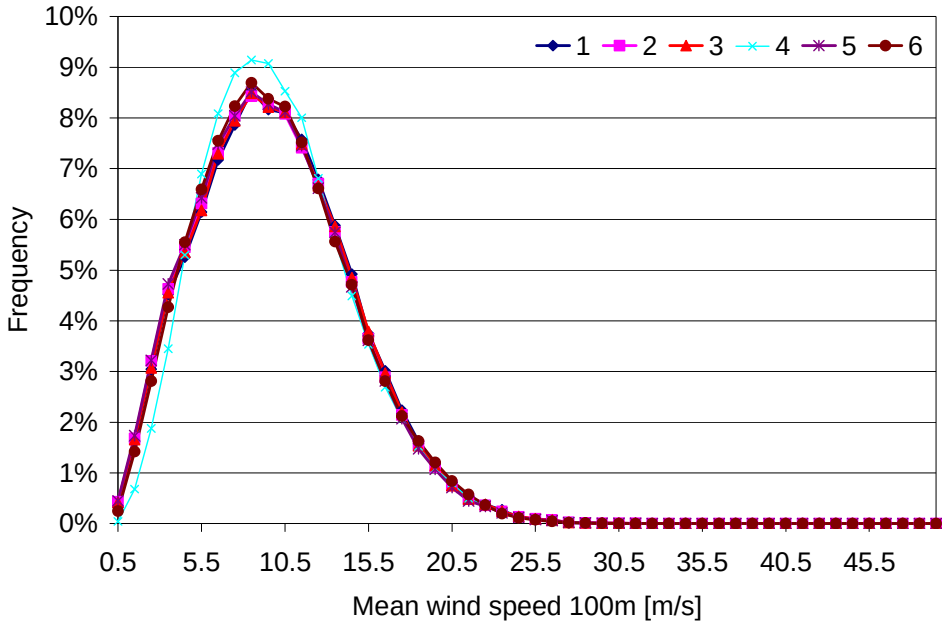

Figure 11.2.2: Long term wind speed frequency distribution at 100 m height level

11.3 Vertical Extrapolation

For the vertical extrapolation all the participants have applied the Hellmann exponential law method. Different values of power law coefficient have been obtained but the final hub height mean wind speed has variations lower than 1%, see Figure 11.3.1.

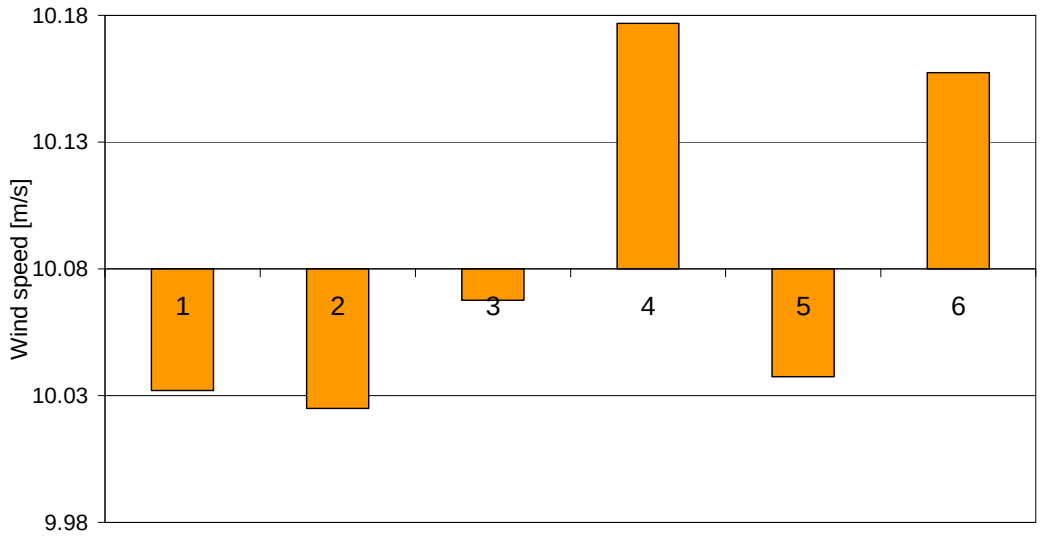

Figure 11.3.1: Hub height mean wind speed obtained from frequency distribution of hours in the year as a function of wind speed and direction. Mean value ± 1%

Figure 11.3.2 shows the hub height frequency wind speed distribution. It is observed that there are slightly more variations from wind speeds between 5.5 to 12.5 m/s than the one appeared in Figure 11.2.2.

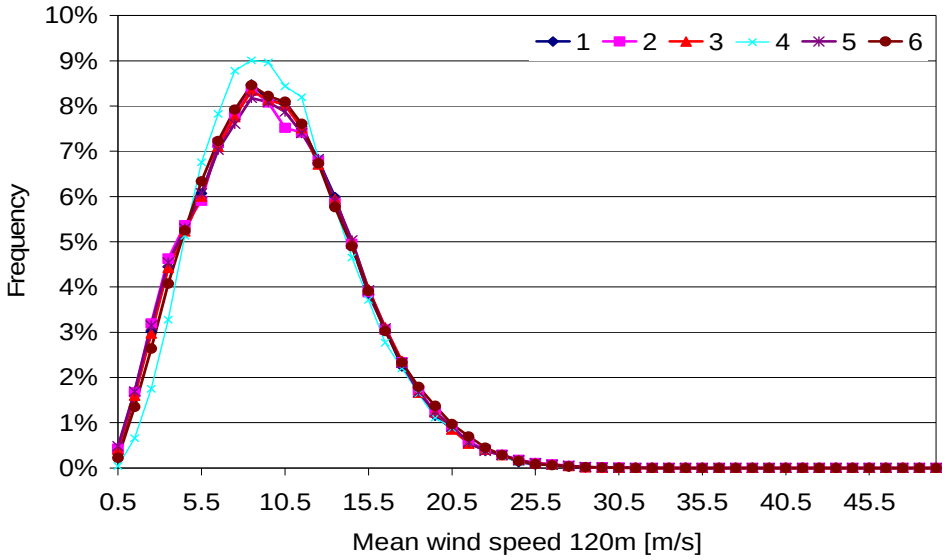

Figure 11.3.2: Hub height wind speed frequency distribution

11.4 Gross Energy (P50)

With the hub height long term wind speed distribution and the power curve, according to the methodologies explained by each participant the gross energy has been estimated, and as Figure 11.4.1 shows the differences between the results increase to a 6.5%.

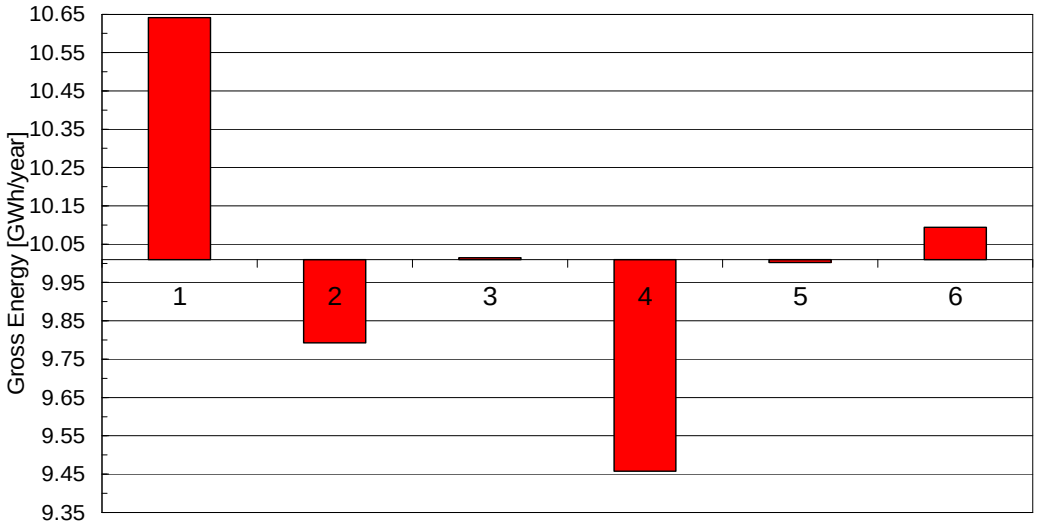

Figure 11.4.1: Gross Energy (P50) at hub height. Mean value ± 6.5%

11.5 Uncertainties and P90

The uncertainties that were taking into account in FINO 1 test case by all the participants have been summarized in Table 11.3. Participant 4 has applied a different methodology to estimate the gross energy so the uncertainties applied are totally different. All most all the participants have considered that there are uncertainties in the Power curve, wind measurements, vertical extrapolation, MCP and time period variability; and all of them have considered that each uncertainty is independent from the others so the final uncertainty is the quadratic sum [11.1] of all the components uncertainties. A Gaussian distribution of the uncertainty is assumed in all cases.

Table 11.3: Summary of the uncertainties consider in the gross energy estimation.

Uncertainty/Participant	1	2	3	4	5	6
Wind measurements	X	X	X	-	X	X
MCP	X	-	X	-	-	X
Variability period used	X	X	X	-	X	X
Vertical extrapolation	X	X	X	-	X	X
Power curve	X	X	X	X	X	X
Propagation of power uncertainty for each ten-minute interval to the total energy production	-	-	-	X	-	-
Statistical error for the energy that is calculated from a sample mean	-	-	-	X	-	-
Air density	X	-	X	-	-	-
Future wind variability 10 year	X	-	X	-	X	X

Figure 11.5.1 shows the uncertainties values estimated in the gross energy calculation. The incidence of the large deviations in the uncertainty value is translated to the gross energy, P90 value, see Figure 11.5.2.

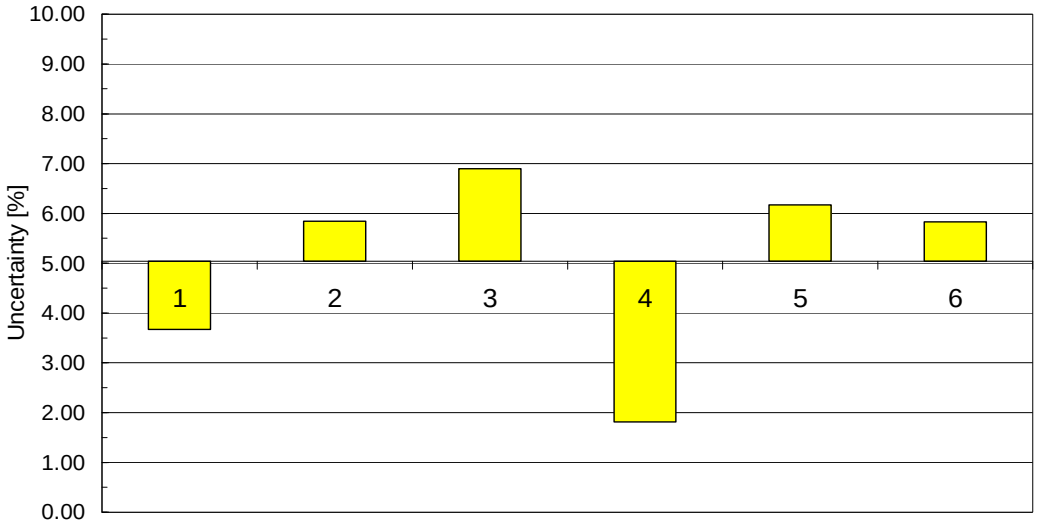

Figure 11.5.1: Gross Energy uncertainty as percentage of P50 value. Mean value ± 100%

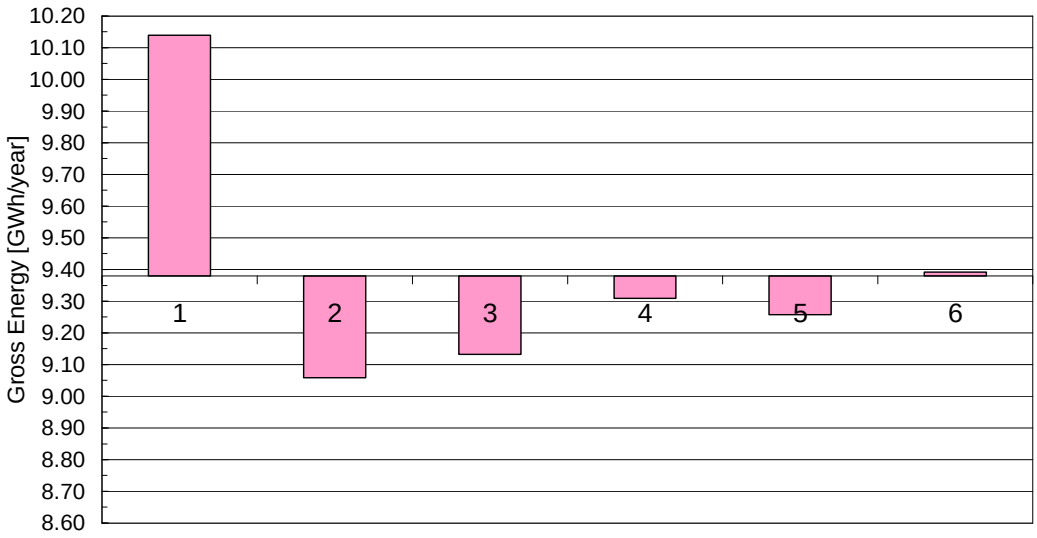

Figure 11.5.2: Gross Energy (P90) at hub height. Mean value ± 8.5%

11.6 Results from Skiron virtual mast

As an alternative to the gross energy estimation from measurements, the same calculation has been done with results from a mesoscale simulation, in this case using Skiron hourly outputs from the period comprehended between June 2003 and January 2013.

With this virtual data, both the data filtered and the vertical extrapolation are not necessary in the energy estimation. Long term extrapolation could be done with reference data, or not, because ten years of simulation are available.

Figure 11.6.1 presents the gross energy (P50) results including two new results, number 7 is the gross energy estimation with 9 years of Skiron simulations and number 8 is the estimation with 32

years, correlating Skiron data with MERRA data to extend the available time period. Both cases are in the same range than the results obtained with measurements.

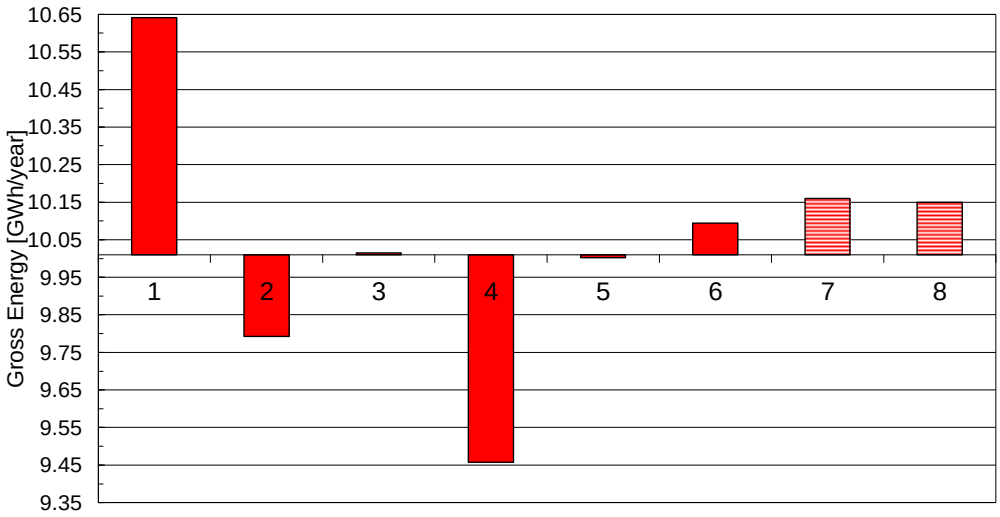

Figure 11.6.1: Gross Energy (P50) at hub height. Including results from virtual data, cases 7 and 8. Mean value ± 6.5%

In the uncertainty estimation the measure and vertical extrapolation uncertainty are replaced by the mesoscale model uncertainty. Figure 11.6.2 shows the effect in the gross energy P90.

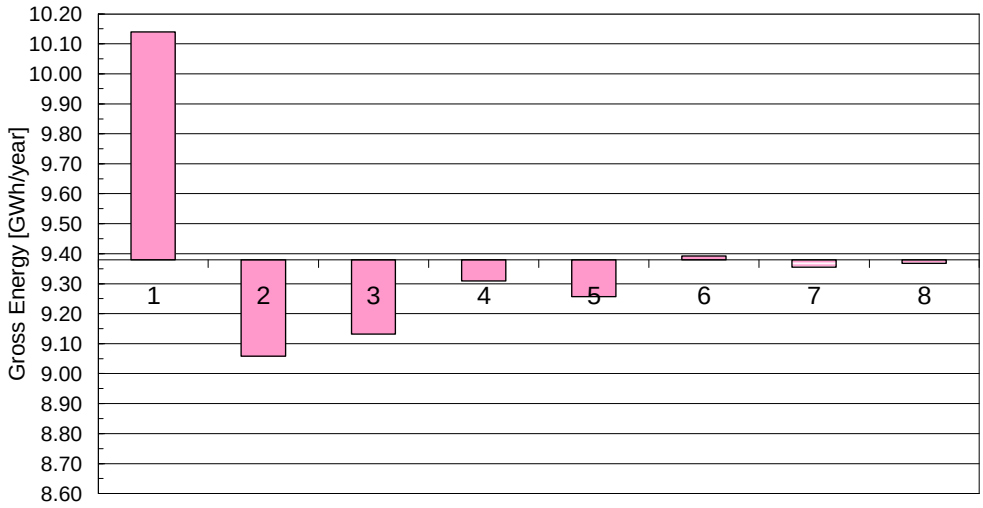

Figure 11.6.2: Gross Energy (P90) at hub height. Mean value ± 8.5%

12 FINO 1 TEST CASE DISCUSSION

In this section after the results obtained in the FINO 1 test case described in point 11 some conclusions and discussion are presented.

According to the steps analyzed in the FINO 1 Gross energy estimation (see Figure 12.1) some critical points have been detected:

- **Filtering:** the large deviations in the data recovery after filtering, mainly due to the mast shadowing effect show the need to have clear rules to filtered erroneous data specially in the case of mast shadowing influence. The data quality checking should be for all the measure period available and after this with all the relevant information select the full year analysis period.
- **Long term:** a great variety of reference data and long term correlation methods are used, in each case and depending on the quality of the available data a exhaustive long term analysis should be done including validation and uncertainty assessment [10.3].
- **Vertical extrapolation:** everybody has used the Hellmann exponential law that has good results for annual mean values but no when profiles are classified in terms of the observed atmospheric stability [12.1] and [12.2], where the wind shear is overestimated during unstable conditions and underestimated in stable conditions. Stability and how it could be applied for wind resource assessment estimation should be analyzed.
- **Gross Energy:** the deviations in the methodologies applied in before steps increasing in the gross energy estimation. According to the results new methodologies, as the explained by FORWIND, should be explored and traditional methodologies should be checked to avoid big discrepancies like in the case of team 1 who with a similar wind speed distribution and the same power curve has obtained higher gross energy than the others participants.
- **Uncertainty:** the sources of the uncertainty are clear but they are not enough to estimate it
- **Virtual masts:** the results obtained for Skiron outputs for the FINO 1 site are very good, but more sites to validate are need to conclude that virtual masts are a alternative for initial offshore wind resource assessment.

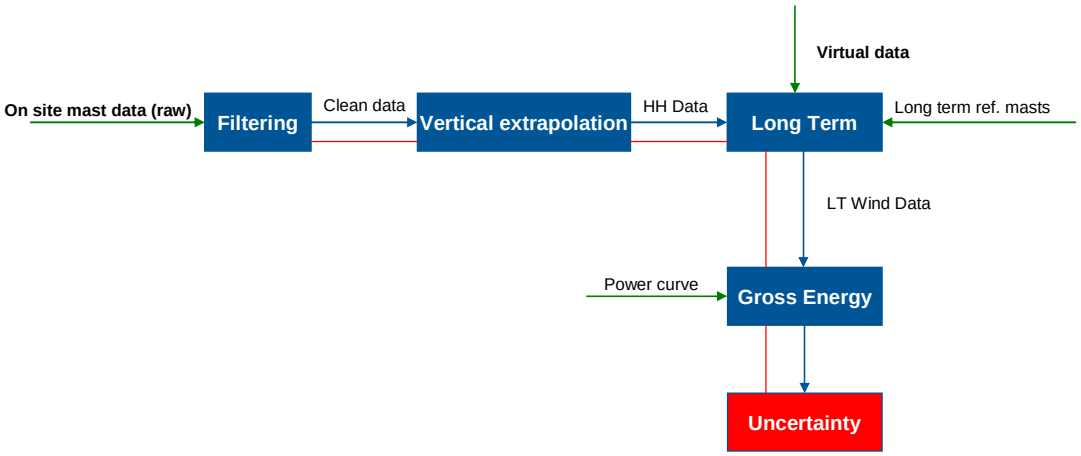

Figure 12.1: Flowchart of the FINO 1 test case composed of a series of modules (blocks), input data (in green) and exchanged variables (black text on blue arrows). The uncertainty estimation followed up all the process (red lines)

According to these results two conclusions are obtained: first, the need of clear and common methodologies and standards to do the wind energy yield assessment in offshore wind farms and second that the NWP outputs are a good source of information to estimate the offshore wind resource.

Extension of the already started work should be comparing the results of energy yield estimation against real wind farm performance data, including in the analysis the wake losses, the electrical losses and the availability losses. This work could be done either with Alpha Ventus Wind Farm if the wind farm performance data would be available or with Horns Rev.

13 AVAILABILITY LOSSES FOR A GENERIC OFFSHORE WIND FARM (RES)

13.1 Introduction

The energy yield lost due to turbines being unable to operate whilst they are being serviced or awaiting repair ('*Turbine Availability Loss*') is one of the most significant loss factors required for an energy yield assessment of an offshore wind farm. It can depend strongly on various factors including the turbine model, maintenance schedules, O&M (Operations and Maintenance) strategy, distance between the wind farm and the O&M base and the wind farm's wind and wave climate.

RES have estimated the energy-based Turbine Availability loss for a generic 600 MW offshore wind farm for a number of scenarios, using the RES software SWARM. The calculated loss encompasses all energy yield losses that result from turbine downtime. This includes time required to obtain replacement parts, travel to the turbines and carry out repairs, downtime due to scheduled servicing and delays caused by bad weather.

SWARM uses Monte Carlo simulations to model the operation and maintenance of a wind farm. It accounts for predicted failure rates, wind and wave conditions, vessel capability and response times, spares holdings and maintenance resources to forecast operational availability. Each simulation is run for a period of 70 years, to produce an annual average Turbine Availability Loss for the wind farm.

13.2 SWARM inputs

The inputs used for the SWARM runs conducted for the EERA DTOC project are described below.

Turbine Layout and Turbine Model

A simple 10 x 10 square wind farm layout was defined, on a regular grid with inter-turbine spacing of seven rotor diameters. Each turbine was defined with a capacity of 6MW and rotor diameter of 154 m and hub height of 100 m. This gives a total capacity of 600 MW.

A generic turbine power curve was used for this work to represent a typical 6 MW offshore wind turbine. This turbine size was chosen as a typical size for offshore projects currently in development.

Site Wave Climate

The time taken to carry out repairs can depend strongly on the wave climate at the site. If large waves are common, this will lead to increased delays and more lost energy as workboats will often be unable to access the wind farm.

This work was carried out for three different sites with varying wave climates, in order to provide results over a large range of conditions. The three sites are summarized in Table 13.1.

Table 13.1: Summary of the three wave climates used for this study. Hs = Significant Wave Height.

Wave Climate Scenario	Description	Mean Wind Speed at 100m [m/s]	% of Time Above Hs Limit	
			1.5 meters	2.0 meters
1	Benign Climate	9.0	16.5%	6.3%
2	Moderate Climate	9.4	21.0%	7.4%
3	Severe Climate	9.5	28.3%	12.6%

Wind and wave data was obtained for each of the three sites covering a period of two years. The wind data was derived using the RES implementation of the WRF mesoscale model. The wave data was downloaded from the CEFAS WaveNet database [13.1]. The data were used as a time-series in the SWARM software and repeated to produce the final 70-year model.

Location of O&M Base

Virtual O&M base locations were defined at various distances from the wind farm centre, from 10 km to 150 km. No real port data were used for this study and all tidal restrictions were ignored.

O&M Strategy

Reasonable values were assumed for turbine failure rates and maintenance schedules. It was assumed that sixty employees would work from and onshore O&M base between the hours of 7 am and 5 pm each day, year-round. The following maintenance vehicle scenarios were considered (see Table 13.2), with increasing operational cost:

1. Five standard workboats, each capable of servicing the wind farm for a significant wave height of up to 1.5 m and carrying twelve passengers
2. Five more advanced workboats, each capable of servicing the wind farm for a significant wave height of up to 2.0 m, also carrying twelve passengers
3. Same as scenario 2, but with the addition of two helicopters, each capable of carrying two passengers.

Workboats were assumed to travel at a speed of 37 km/h, with helicopters travelling at 240 km/h. For each case, it was assumed that one jack-up vessel would be available with a lead time of 30 days.

Table 13.2: Parameters for the three O&M scenarios.

Scenario	Number of Workboats	Number of Helicopters	Wave Hs Limit for Boats [m]
1	5	0	1.5
2	5	0	2.0
3	5	2	2.0

13.3 Definition of '*Excess turbine availability loss*'

The SWARM software produces an estimate of the overall percentage of energy lost due to turbine downtime. These results will depend strongly on the assumptions of turbine failure rates, response times and amount of spare parts held at the O&M base. In order to remove some of these dependencies, the results presented here have been normalized relative to a base-case result.

The base-case used here has the following properties:

1. O&M base is at the centre of the wind farm
2. Five workboats with no operational restrictions (i.e. no waves)
3. Same layout and turbine type as described above

The base-case availability loss is therefore the loss that would be seen with minimal travel time to the wind farm and with a perfectly calm sea. For real wind farm scenarios, any additional loss caused by increased travel time and/or high waves is referred to in this study as '*Excess Turbine Availability Loss*'.

In general, the results presented here are intended to be used comparatively, i.e. to understand the difference in availability that could be expected with different scenarios. However, anyone wishing to use these results to calculate an absolute Turbine Availability Loss should first define their own base-case availability loss and combine it with the Excess Turbine Availability Loss provided here. The losses should be combined multiplicatively, as follows:

(1-Total Turbine Availability Loss) = (1-Base Case Loss) x (1-Excess Turbine Availability Loss)

13.4 Excess turbine availability loss: Results

The following tables (Table 13.3, Table 13.4 and Table 13.5) show the calculated Excess Turbine Availability Loss for the range of scenarios considered. The loss can be seen to vary from 0.5% to 10.2%, depending on the O&M strategy, wave climate and distance from the O&M base. Results are also presented in Figure 13.4.1.

All losses are given as a percentage of energy yield. They are therefore 'energy-based' losses, rather than the 'time based' losses that are sometimes used.

Table 13.3: O&M Scenario 1: Five workboats, Hs limit = 1.5m.

Distance from O&M base [km]	Wave Climate		
	Benign	Moderate	Severe
10	1.2%	1.4%	2.9%
20	1.3%	1.5%	3.0%
40	1.8%	2.0%	3.9%
60	2.2%	2.5%	4.8%
80	2.7%	2.9%	6.0%
100	3.1%	3.6%	6.9%
150	5.2%	6.0%	10.2%

Table 13.4: O&M Scenario 2: Five workboats, Hs limit = 2.0 m.

Distance from O&M base [km]	Wave Climate		
	Benign	Moderate	Severe
10	0.5%	0.7%	1.2%
20	0.6%	0.8%	1.3%
40	0.9%	1.1%	1.7%
60	1.1%	1.3%	2.2%
80	1.3%	1.6%	2.7%
100	1.7%	2.1%	3.3%
150	2.9%	3.6%	5.1%

Table 13.5: O&M Scenario 3: Five workboats, Hs limit = 2.0 m, with 2 helicopters

Distance from O&M base [km]	Wave Climate		
	Benign	Moderate	Severe
10	0.5%	0.6%	0.7%
20	0.6%	0.7%	0.8%
40	0.8%	1.0%	1.2%
60	1.1%	1.3%	1.7%
80	1.4%	1.6%	2.2%
100	1.7%	2.0%	2.9%
150	3.0%	3.6%	4.8%

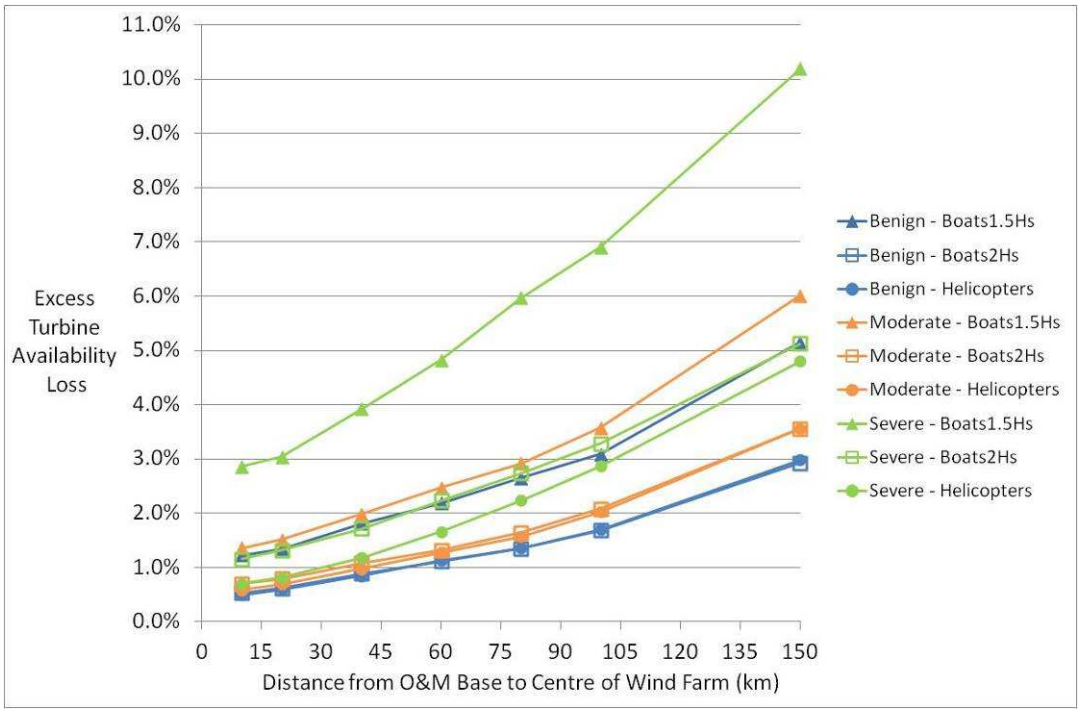

Figure 13.4.1: Energy-based Excess Turbine Availability Loss results for the range of scenarios considered in this study. This is the percentage of energy yield lost due to time taken to travel to the wind farm to make repairs and time lost due to high waves.

As described in Section 13.3, to derive a total loss due to turbine downtime a base Turbine Availability loss must be included in combination with the losses shown in Figure 13.4.1.

Sensitivity of Results to Input Data

The results of the SWARM simulations are heavily dependent on the input data. This study has aimed to cover a wide range of site conditions and O&M strategies, but the availability for a real wind farm will depend on the precise combination of a wide variety of factors.

The results will be broadly valid for wind farms of different capacities. For example, similar results could be expected for a wind farm twice the size at 1.2GW, provided that the numbers of workboats and workforce were increased accordingly.

A change to the turbine model (i.e. different rotor diameter, hub height or rated power) will have an impact on the appropriate failure rates and the amount of energy lost by any particular period of downtime. Therefore, using a significantly different turbine model is likely to impact the absolute availability losses derived here. However, the relative availability losses between scenarios and the general trends shown in Figure 13.4.1 should remain broadly similar.

The largest impact on availability will be seen if the O&M strategy is different to those used here, or for sites where the wind climate is significantly different from the three scenarios considered. For example, for sites far offshore it is possible that an offshore O&M base would be constructed, which would significantly reduce the losses due to travel time.

13.5 Conclusions

This study has estimated the loss due to turbine downtime for a generic 600MW offshore wind farm. This has been presented as an Excess Turbine Availability Loss, which is the extra loss caused by travel time to the site and high waves, over and above the base-case availability loss expected for a site with no waves and minimal travel time.

Results show that the Excess Turbine Availability Loss varies between 0.5% and 10.2% depending on the scenario considered.

The results are intended to be used in order to compare different wind farm strategies rather than as absolute energy yield loss factors.

14 O&M TOOLS (ECN)

14.1 ECN O&M Tool

14.1.1 The Software

The ECN O&M Tool Version 4, see Figure 14.1.1 has been developed to estimate the long term annual average costs and downtime of an offshore wind farm. The O&M tool should be used in the planning phase of a wind farm. By means of "what-if analyses" project developers are able to compare the adequacy of different maintenance strategies with each other. Parameters like the reliability of components, usage and costs of vessels and weather conditions can be changed very easily and the program responds with cost and availability figures per year and per season.

Figure 14.1.1 ECN O&M Tool.

14.1.2 The Model

The ECN O&M Tool is implemented in MS-Excel and consists of three modules:

1. WaitingTime> This module analyses the wind and wave conditions and for each type of equipment the module determines the waiting time as a function of the mission time, which is expressed as a simple polynomial function.
2. CostCal> In this module the costs and downtime for a certain wind farm with a certain O&M scenario are being calculated.
3. Application> With this module the user can determine how many vessels and labour are needed in every season (and is new as compared to the previous versions of the ECN O&M Tool).

The tool uses long term average data as input (failure rates, wind and wave statistics, costs of vessels and spare parts, lead time of vessels and spare parts, etc.) and generates long term average values as output (costs, downtime, and required resources). Based on the results of the baseline scenario, cost drivers can be identified and by means of scenario studies the optimal strategy can be determined. The add-in module "@Risk" can be used to carry out uncertainty analyses once the optimal strategy is determined and to check the robustness of the output.

The tool functions very straightforwardly as it are programmed in MS-Excel. Each change in the input parameters immediately results in a change of the output parameters. Most users appreciate the openness of the software and consider the tool very user-friendly. The tool includes generated tables, pie charts and bar charts to identify the drivers for costs and downtime and to assist in defining an improved strategy.

The model requires an extensive list of input parameters and a detailed description of the proposed O&M strategy. By doing so, the tool forces the user to consider all aspects relevant for O&M in large detail. During the process of defining the baseline O&M strategy and collecting the required input data, users are often confronted with the fact that only little information on e.g. failure rates and capabilities of vessels is known in the planning phase. Most users of the ECN O&M Tool consider the process of discussing the O&M approach in detail and finding agreement on the assumptions and input parameters equally important to the model output itself!

14.1.3 The Experience

In 2007, the tool received a validation statement from Germanischer Lloyd, which makes it the only software validated worldwide for analysing O&M aspects! More than 20 leading project developers, manufacturers of offshore wind turbines, and consultants make use of the tool, and for many European offshore wind farms cost efficient O&M strategies have been developed with the tool. The results of the analyses are accepted by financers and due diligence. Every year the users of the tool meet during the annual user day meetings and a.o. they give feedback about the tool. ECN has incorporated their recommendations in Version 4.

14.2 OMCE Calculator

14.2.1 The Software

The OMCE-Calculator (Operation and Maintenance Cost Estimator) [14.1] has been developed to estimate the future O&M costs of an operating offshore wind farm. The OMCE-Calculator can be used for estimating required O&M budgets for the next say 1, 2, or 5 years. Such a situation is relevant for instance at the end of the warranty period, or when new contracts with OEM's and/or contractors need to be extended.

The OMCE-Calculator requires details on preventive, corrective and condition based maintenance as input for the wind turbines as well as for the Balance of Plant (BOP). The tool is best used with operational data from the wind farm under consideration, but can also be used with long term average data as input (failure rates, wind and wave statistics, costs of vessels and spare parts, lead time of vessels and spare parts, etc.).

The tool responds with cost and availability figures and generates tables with figures and graphs that can be used for optimisation purposes see Figure 14.2.1. By means of "what-if analyses" (How much does the downtime reduce if I use more vessels or keep less spares in stock?) the wind farm operators are able to compare the adequacy of different maintenance strategies and to select the most cost effective one. Since the OMCE-Calculator is a time simulation tool, it automatically incorporates the variability due to weather conditions and random occurrence of failures.

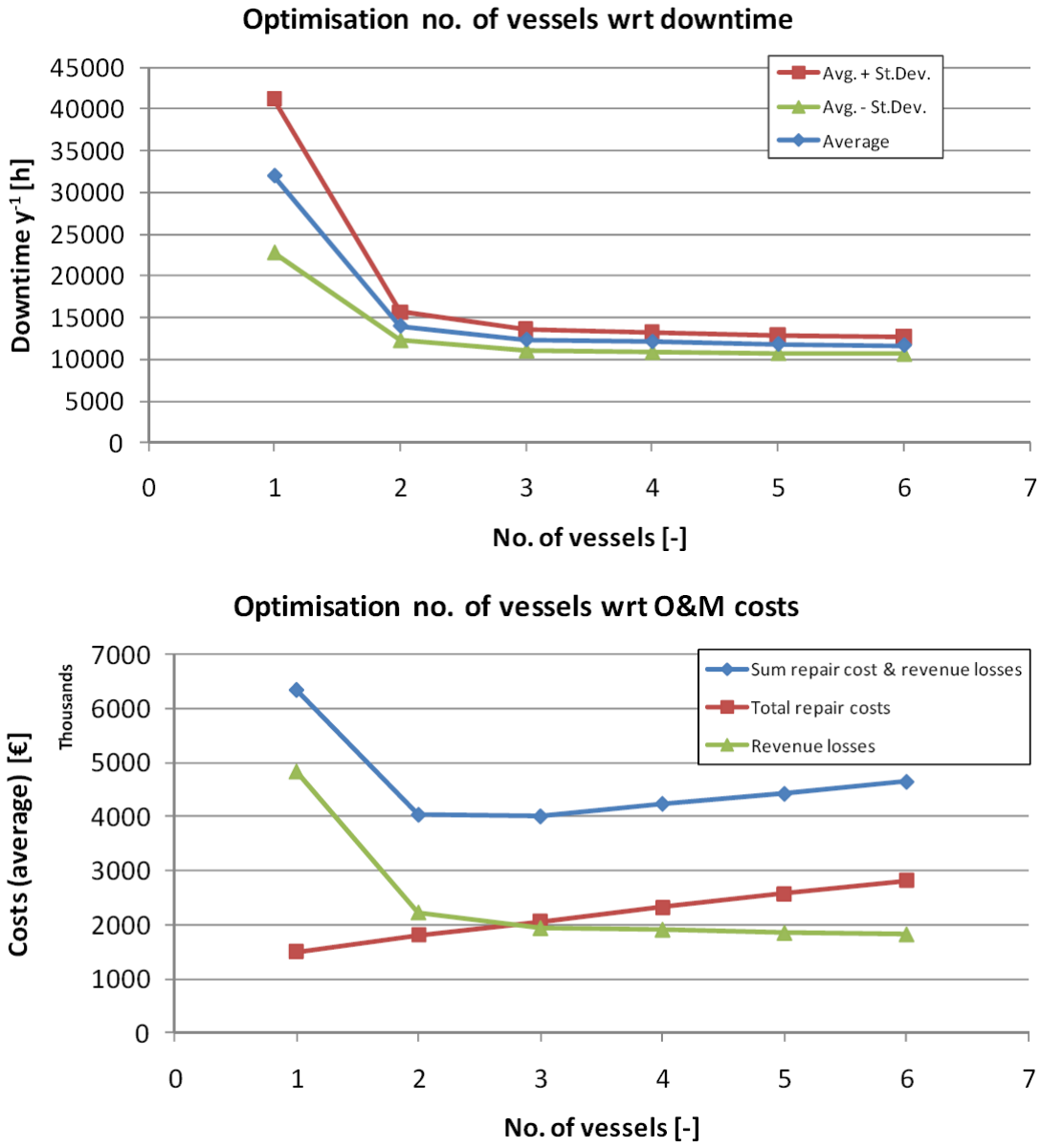

Figure 14.2.1: Example of figures generated by OMCE Calculator. At the top results of variation of no. of available vessels vs. total downtime of wind turbines; At the bottom sum of total O&M cost and revenue losses as a function of no. of available vessels

14.2.2 The Model

The OMCE-Calculator is a time domain simulation tool built with MATLAB and designed with user-friendliness in mind. The tool consists of four modules:

1. Input: The graphic user interface (GUI) is designed to facilitate the user in defining the baseline O&M scenario and the successive improvements.
2. Pre-processor: The O&M models and weather data are pre-processed to assess the accessibility of the defined equipment and their weather limits.

3. Simulator: The maintenance schemes are integrated in time for the defined O&M scenario by performing a number of simulations for a user-defined period in the near-future.
4. Post-processor: Costs are assigned to the simulated maintenance schemes and downtime results. The results are presented in tables and graphs.

The four modules are usually executed in order, and are all accessible from the OMCE-Calculator main menu. The tool generates averages, standard deviations and minima/maxima as output for the user-defined period (costs, downtime, and required resources). Based on the results of the baseline scenario, cost drivers can be identified and by means of scenario studies the optimal strategy can be determined.

15 POWER CURVE DEVIATIONS (FORWIND)

A power curve provides a relation between the wind inflow and the electrical power output of a wind turbine. It is therefore one of the central characteristics of the machine and of major importance for both turbine manufacturers and wind farm operators.

As a crucial problem of wind turbine performance testing, for full-size wind turbines there is no possibility to conduct tests in controlled wind conditions. To handle this specific difficulty and to allow for unified performance testing, the international standard IEC 61400-12-1 [8.4] has been worked out. It defines measurement and data analysis procedures which lead to a standardized power curve. As central components, the wind measurement is required at hub height of the machine and in a distance of 2.5 to 4 rotor diameters, and both wind and power measurements are analysed using ten-minute mean values. An underlying assumption of a uniform wind inflow justifies this procedure, but cannot be ensured in field measurements.

While the power curve is meant to be turbine specific, a dependence on the site-specific wind conditions could not be avoided in the standard. Namely, the power curve will depend on the wind shear during the measurement, i.e., the shape of the vertical wind profile, and on the turbulence intensity. Both effects stem from the non-linear shape of a typical power curve. The approximately cubic dependency of power on wind speed in the partial load regime leads to large gains of power from the higher wind speeds in height levels above hub height, which are not balanced by losses in lower height levels. Accordingly, an increased turbulence level leads to power gains during moments of higher wind speeds, which are not balanced by the losses in moments of lower wind speeds. Consequently both higher wind shear and turbulence would lead to an increase in power values of the power curve. Further effects, such as flow distortion due to terrain topography, may also influence the power characteristics. These considerations become even more significant with the increasing rotor diameters of recent wind turbines, which cover larger and larger areas and contradict even more the intrinsic assumption of a uniform wind inflow.

For practical reasons, power curves are typically measured by the manufacturer in an onshore site. Moreover, the standards IEC 61400-12 are restricted to onshore sites. For offshore sites typically reduced shear and turbulence levels are found due to the rather flat sea surface, compared to onshore sites. Therefore a power curve measured offshore will typically show lower power levels than that of an onshore site, even if measured for identical turbine models. It should nevertheless be noted that the overall energy yield gained offshore is generally higher than onshore, due to significantly higher average wind speeds.

Summarizing, it can be concluded that deviations between manufacturer and on-site power curves are frequently found, even when all measurements and analyses strictly follow the standards. As a main cause of these deviations differences in the wind conditions can be identified. Especially offshore sites generally show reduced levels of vertical shear and turbulence intensity. Therefore a power curve measured offshore typically deviates from an onshore measurement at an identical turbine, with a tendency towards lower power values.

16 CONCLUSIONS

The FINO 1 test case demonstrate the need of clear and common methodologies and standards to do the wind energy yield assessment in offshore wind farms; in this context a start point to define good practices is the MEASNET guideline *" Evaluation of site specific wind conditions"* [9.2] which provides the definition of methodology and requirements for a site assessment procedure.

New methodologies should be explored and incorporate to the wind energy yield assessment, like the analysis of atmospheric stability to define the wind profile or the NWP outputs as source of information to estimate the offshore wind resource.

To develop and validate methodologies and procedures wind farm data are need.

The loss due to turbine downtime for a generic 600MW offshore wind farm has been estimated. This has been presented as an Excess Turbine Availability Loss, which is the extra loss caused by travel time to the site and high waves, over and above the base-case availability loss expected for a site with no waves and minimal travel time.

The results are intended to be used in order to compare different wind farm strategies rather than as absolute energy yield loss factors.

It is recommended that as extension of the already started work a comparison of the results of energy yield estimation against real wind farm performance data, including in the analysis the wake losses, the electrical losses and the availability losses will be done. This work could be done either with Alpha Ventus Wind Farm if the wind farm performance data would be available or with Horns Rev.

Finally, it is recommend work in how estimate clearly the uncertainty associated to each step in the energy yield assessment procedure.

17 REFERENCES

[3.1] "sensor_readme_111026.pdf" sent by BSH

[3.2] http://www.bsh.de/en/Marine_data/Projects/FINO/index.jsp

[3.3] T. Neumann, K. Nolopp (2007) Three Years Operation of Far Offshore Measurements at FINO1. DEWI Magazin 30: 42-46, February 2007

[5.1] P.A. Jimenez, J.F. Gonzalez-Rouco, J. Navarro, J.P. Montavez and E. Garcia-Bustamante, 2010: Quality assurance of surface wind observations from automated weather stations. J. Atmospheric & Oceanic Technology, 27, 1101 – 1122.

[5.2] A. Westerhellweg, T. Neumann and V. Riedel, 2012: FINO1 Mast Correction. Dewi magazin nº. 40, 60 - 66.

[7.1] IEC: IEC61400-1 Wind turbines - Part 1: Design Requirements, 3rd Ed., 2005.

[8.1] A. M. S. Karagali Ioanna and C. B. Hasager, Analysis of 10 years of wind vector information from quikscat for the North Sea: Preliminary results from the orec-ca project, EWEA 2011 Proceedings, 2011

[8.2] V. R. A. Westerhellweg, T. Neumann, Fino 1 mast correction, DEWI Magazin, 40 (2012), pp. 60-66

[8.3] P. Milan, M. Wächter, and J. Peinke, "Stochastic modeling of wind power production," in Proceedings of EWEA 2011, (Brussels), 2011.

[8.4] IEC: IEC61400-12-1 Wind turbines - Part 12-1: Power performance measurements of electricity producing wind turbines, 1st Ed., 2005.

[9.1] http://www.windographer.com/

[9.2] MEASNET: Evaluation of site specific wind conditions, Version 1 November 2009

[9.3] A.L. Rogers, J.W. Rogers, J.F. Manwell (2005) 'Comparison of the performance of four measure-correlate-predict algorithms', Journal of Wind Engineering and Industrial Aerodynamics, 93 243–264

[9.4] P. van Lieshout (2010) 'Improvements in AEP Calculations Using IEC 61400', Windtech International, 6 (3)

[9.5] C. King , B. Hurley (2005) 'The SpeedSort, DynaSort, and Scatter wind correlation methods', Wind Engineering, 29, 3, 217-241

[9.6] M. Leblanc, D. Schoborg, S. Cox , A. Haché, and A. Tindal (2009) 'Is a non-linear MCP method a useful tool for North American wind regimes?', *Proceedings of the WINDPOWER 2009 Conference*, Chicago, Illinois, USA

[9.7] M. Anderson, J. Bass (2004) 'A review of MCP techniques', Renewable Energy Systems Ltd, Report No. 01327R00022, Issue No.3

[9.8] T. Lambert, A. Grue (2012) 'The Matrix Time Series method for MCP', *Proceedings of the WINDPOWER 2012 Conference*, Atlanta, Georgia, USA

[9.9] F. Bañuelos-Ruedas, C. A. Camacho, S. Rios-Marcuello (2011) Methodologies Used in the Extrapolation of Wind Speed Data at Different Heights and Its Impact in the Wind Energy Resource

Assessment in a Region, Wind Farm - Technical Regulations, Potential Estimation and Siting Assessment, Dr. Gastón Orlando Suvire (Ed.)

[9.10] G.L. Johnson, Wind Energy Systems. (December of 2006) Electronic Edition. http://www.eece.ksu.edu/~gjohnson/Windbook.pdf. Accesed May 2010.

[9.11] J. F. Manwell, J. G. McGowan, and A. Rogers (2002) Wind Energy Explained, John Wiley & Sons Limited.

[9.12] IEA: IEA Recommendation 11: Wind Speed Measurement and Use of Cup Anemometry, 1st Ed., 1999.

[9.13] TrueWind Solutions, (February 2003) "Wind Energy Resource Maps of the Republic of Ireland".

[10.1] G.L. Mellor, G.T. Yamada, 1982, Development of a Turbulence Closure Model for Geophysical Fluid Problems, Rev. Geophys. Space Phys. 20: 851-875.

[10.2] C.A. Paulson (1970). The mathematical representation of wind speed and temperature profiles in the unstable atmospheric boundary layer. J. Appl. Meteorol. 9: 857-861.

[10.3] MEASNET, Evaluation of Site-Specific Wind Conditions, Version 1, November 2009.

[11.1] ISO/IEC Guide 98:1995 - Guide to the Expression of uncertainty in measurement, Geneva, Switzerland.

[12.1] Sanz Rodrigo J (2011) Flux-profile characterization of the offshore ABL for the parameterization of CFD models. EWEA Offshore 2013, Amsterdam, November 2011

[12.2] Lozano S, Sanz Rodrigo J (2013) Evaluation of Skiron mesoscale model at Fino-1 as a function of atmospheric stability. ICOWES 2013, Copenhagen, June 2013

[13.1] http://cefasmapping.defra.gov.uk/Map

[14.1] H. Braam, T.S, Obdam, R.P. Van de Pieterman, L.W.M.M. Radermakers

18 ANNEX 1: SENSOR DESCRIPTION

	Sensor position with respect to centre of mast				Sensor alignment	Parameter	Installation at	Sensor type
Name	**x [m]**	**y [m]**	**z [m]**	**alpha [°]**	Description			
	Directing from centre of mast towards **NE**	Directing from centre of mast towards **NW**	Height **LAT**	Position of sensor with respect to centre of mast (angle from N) or: Direction under which the sensor can be seen from centre of mast (origin)	Wind sensors: Direction of north mark with respect to sensor axis (angle from N) Radiation and rain sensors: orientation with respect to horizontal plain (H = horizontal)			

Name	Sensor position with respect to centre of mast				Sensor alignment	Parameter	Installation at	Sensor type
	x [m]	y [m]	z [m]	alpha [°]	Description			
v(100)	0	0	103	-	-	Wind speed	Telescope bar	Vector A100LM-WR-PC3 Cup Anemometer
hygro(100)			101	-	-	Humidity	Supporting frame	Thies Hygro- Thermo Transmitter 1.1005.50.512
temp(100)			101	-	-	Air temperature		
v(90)	0	-3.7	91.5	135	-	Wind speed	Bracket SE	Vector A100LK-WR-PC3 Cup Anemometer
dir(90)	0	3.7	91.5	315	45	Wind direction	Bracket NW	Thies Wind Vane Classic 4.3120.22.012
rain(90)			101		H	Precipitation	Supporting frame	Thies Precipitation Monitor 5.4103.10.000
pyrano(90)			91.5		H	Global radiation	Bracket	Kipp & Zonen Pyranometer CM11
UV(90)			91.5		H	UV radiation	Bracket	Kipp & Zonen CUV3
v(80)	-0.3	-3.9	81.5	139	-	Wind speed	Bracket SE	Vector A100LK-WR-PC3 Cup Anemometer
USA(80)_u	-0.3	3.9	81.5		until 2006-07-06 11:30:00: **331** since 2006-07-06 11:30:00: **11**	Wind vector u	Bracket NW	Gill R3-50 Ultrasonic anemometer
USA(80)_v	-0.3	3.9	81.5	311		Wind vector v		
USA(80)_w	-0.3	3.9	81.5			Wind vector w		
v(70)	-0.7	-5.06	71.5	143	-	Wind speed	Bracket SE	Vektor A100 -LM -WR -PC3 Cup Anemometer
dir(70)	-0.7	5.06	71.5	307	40	Wind direction	Bracket NW	Thies Wind Vane Classic 4.3120.22.012
temp(70)			72	-	-	Air temperature	Supporting frame	Thies Thermo Transmitter
v(60)	-0.74	-5.75	61.5	142	-	Wind speed	Bracket SE	Vector A100LK-WR-PC3 Cup Anemometer
USA(60)_u	-0.74	5.75	61.5		until 2006-07-06 11:30:00: **83** since 2007-02-01 09:26:23: **23.5**	Wind vector u	Bracket NW	Gill R3-50 Ultrasonic anemometer
USA(60)_v	-0.74	5.75	61.5	308		Wind vector v		
USA(60)_w	-0.74	5.75	61.5			Wind vector w		
v(50)	-0.6	-7	51.5	140	-	Wind speed	Bracket SE	Vector A100LK-WR-PC3 Cup Anemometer
dir(50)	-0.6	7	51.5	310	123.5	Wind direction	Bracket NW	Thies Wind Vane Classic 4.3120.22.012
temp(50)			52	-	-	Air temperature	Supporting frame	Thies Hygro- Thermo Transmitter 1.1005.50.512
hygro(50)			52	-	-	Humidity		
v(40)	-1	-8.2	41.5	142	-	Wind speed	Bracket SE	Vector A100LK-WR-PC3 Cup Anemometer
USA(40)_u	-1	8.2	41.5		until 2006-07-06 11:30:00: **306** since 2006-07-06 11:30:00: **252.5**	Wind vector u	Bracket NW	Gill R3-50 Ultrasonic anemometer
USA(40)_v	-1	8.2	41.5	308		Wind vector v		
USA(40)_w	-1	8.2	41.5			Wind vector w		
temp(40)			42	-	-	Air temperature	Supporting frame	Thies Thermo Transmitter

v(30)	-1.15	-8.35	34	143	-	Wind speed	Bracket SE	Vector A100LK-WR-PC3 Cup Anemometer
dir(30)	-1.15	8.35	34	307	43	Wind direction	Bracket NW	Thies Wind Vane Classic 4.3120.22.012
hygro(30)			34.5	-	-	humidity	Supporting frame	Thies Hygro- Thermo Transmitter 1.1005.50.512
temp(30)			34.5	-	-	Air temperature		
pyrano(30)			34.5	SW	H	Global radiation	Bracket SW	Kipp & Zonen Pyranometer CM11
rain(20)			23.5	-	H	Precipitation	outside measurement-container	Thies Precipitation Sensor 5.4103.20.xxx
baro(20)			22.5	-	-	Air pressure		Vaisala Baro Transmitter PTB 100 A

Sensor	Manufacturer		
	Name	**Address**	**State**
Cup anemometer	Vector Instruments	115 Marsh Road,Ryhl, Denbighshire LL18 2AB	UK
Ultrasonic anemometer	Gill Instruments	Saltmarsh Park 67 Gosport Street,Lymington, Hampshire SO41 9EG	UK
Wind vane Thermo- Hygro Transmitter Thermo Transmitter Precipitation monitor Precipitation sensor	Adolf Thies GmbH&Co.KG	Hauptstr.76, 37083 Göttingen	Germany
Baro transmitter	Vaisala	P.O.Box 26, FIN-00421 Helsinki	Finland
Pyranometer UV sensor	Kipp&Zonen	Röntgenweg 1, 2624 BD Delft	The Netherlands
Lightning detector	meteorlabor ag	Hofstr. 92 CH-8620 Wetzikon 1	Switzerland
Accelerometer (deck & mast)	Endevco Corporation	30700 Rancho Viejo Road, San Juan, CA 92675	USA
Accelerometer (Jacket) Strain gauges	Hottinger Baldwin Messtechnik GmbH	Im Tiefen See 45, 64293 Darmstadt	Germany